Summer 8-31-2003

A combined channel-modified adaptive array MMSE canceller and viterbi equalizer

Richard M. Friedman
New Jersey Institute of Technology

ABSTRACT

A COMBINED CHANNEL-MODIFIED ADAPTIVE ARRAY MMSE CANCELLER AND VITERBI EQUALIZER

by
Richard M Friedman

In this thesis, a very simple scheme is proposed which couples a maximum-likelihood sequence estimator (MLSE) with a X-element canceller. The method makes use of the MLSE's channel estimator to modify the locally generated training sequence used to calculate the antenna array weights. This method will increase the array's degree of freedom for interference cancellation by allowing the dispersive, desired signal to pass through the array undisturbed. Temporal equalization of the desired signal is then accomplished using maximum-likelihood sequence estimation. The T-spaced channel estimator coefficients and the array weights are obtained simultaneously using the minimum mean square error criteria. The result is a X-element receiver structure capable of canceling X-1 in-band interferences without compromising temporal equalization.

A COMBINED CHANNEL-MODIFIED ADAPTIVE ARRAY MMSE CANCELLER AND VITERBI EQUALIZER

by
Richard M Friedman

A Thesis
Submitted to the Faculty of
New Jersey Institute of Technology
In Partial Fulfillment of the Requirements for the Degree of
Master of Science in Electrical Engineering

Department of Electrical and Computer Engineering

August 2003

APPROVAL PAGE

A COMBINED CHANNEL-MODIFIED ADAPTIVE ARRAY MMSE CANCELLER / VITERBI EQUALIZER

Richard M Friedman

Dr Yeshkel Bar-Ness, Thesis Advisor — Date
Distinguished Professor, Department of Electrical and Computer Engineering, NJIT

Dr Alexander Haimovich , Committee Member — Date
Professor, Department of Electrical and Computer Engineering, NJIT

Dr Ali Abdi, Committee Member — Date
Assistant Professor, Department of Electrical and Computer Engineering, NJIT

BIOGRAPHICAL SKETCH

Author: Richard M Friedman

Degree: Master of Science

Date: May 2003

Undergraduate and Graduate Education:

- Master of Science in Electrical Engineering,
  New Jersey Institute of Technology, Newark, NJ, 2003

- Bachelor of Science in Electrical Engineering,
  New Jersey Institute of Technology, Newark, NJ, 1993

Major: Electrical Engineering

Presentations and Publications:

R. Friedman, Y. BarNess, "Combined Channel Modified Adaptive Array MMSE Canceller and Viterbi Equalizer for Interference with Delay Spread," VTC 2001 Spring, pp. 209-213, Rhodes Island, Greece, May 6-9, 2001.

R. Friedman, Y. BarNess, "Combined Channel Modified Adaptive Array MMSE Canceller and Viterbi Equalizer," ISSSTA 2002, Prague, Czech Republic, Sept., 2002.

This thesis is dedicated to my Mother and Sister, who have instilled in me the inquisitive nature and work ethic which was necessary to complete this epic. Thank you both!

ACKNOWLEDGMENT

I would like to thank Dr. Bar-Ness for having remarkable patience with me during the writing of this thesis, and for supplying me with invaluable in-site into the subject matter. I would also like to thank my committee members for their time an effort spent reviewing this work. Also a special thank you is in order for my fellow students, especially Christian Ibaris, Howard Tang, and others for helping me through the years.

TABLE OF CONTENTS

TABLE OF CONTENTS
(Continued)

LIST OF FIGURES

LIST OF FIGURES
(Continued)

Figure **Page**

LIST OF FIGURES
(Continued)

Figure **Page**

CHAPTER 1

INTRODUCTION

The achievable capacity and quality in a narrowband mobile cellular environment is limited by three major environmental impairments. Even though there is other factors which effect system performance, signal fading, interference, and multi-path propagation are the dominant impairments. Interference is mainly in the form of co-channel users being serviced by base stations in close proximity to the end user's location. At the same time, the signal from the servicing base station can undergo both fading and multi-path propagation due to the topology and morphology of the environment the mobile traverses. An example of how these impairments can come about is shown in Figure 1.1. The result to the desired signal from the latter two environmental impairments is a time domain spreading of the information signal referred to as time dispersion, and a complex amplitude variation referred to as fading.

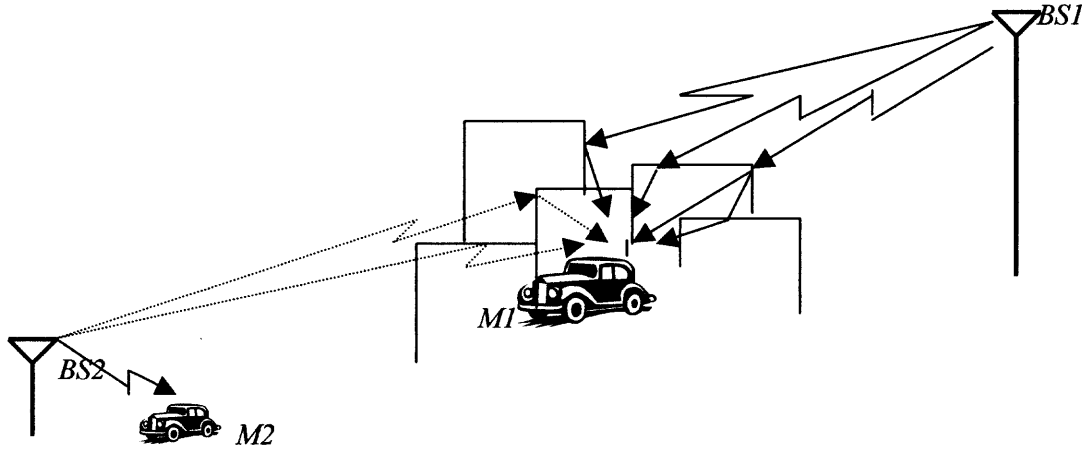

Figure 1.1 The Mobile Radio Environment.

When faded multi-path waveforms arrive at the mobile, they form a composite signal that distorts the desired information-bearing signal. Without a method to neutralize environmental impairments that affect the desired signal, the system's performance will be degraded. In Figure 1.2, a graph is shown which illustrates the limiting effect these impairments have on the bit error rate (BER) of an IS136 digital mobile system. As an example, in Figure 1.2 one can see that multi-path propagation can have a limiting effect on the receiver's BER. This error floor effect is a critical issue that must be dealt with to assure the end-user good quality of service over the entire service network.

The need to combat environmental impairments has been the topic of much research. Much of the work suggests using multiple antennas to combat signal fading and to cancel interference, along with some form of equalization to reduce the affect of multi-path propagation. Since these structures work on the observed signals in the temporal and spatial domains, they can all be generalized as some form of space-time processor (STP).

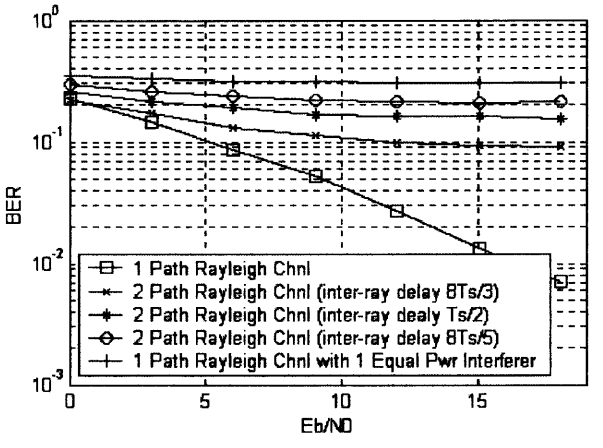

Figure 1.2 Error floor effect for $\pi/4$ DQPSK. Two equal power rays, f_{max}=180 Hz.

1.1 Linear Space-Time Processing

There are a variety of space-time receiver structures. Each STP is derived using some form of optimization criteria, as well as assumptions on which environmental impairments will be dominant. The choice of optimization criteria and environmental factors one assumes govern the resultant design. As an example, in [24] the author shows that by weighting each element in a mobile antenna array by it's local signal to noise ratio (SNIR), then summing across the array, the SNIR at the array's output can be maximized. The technique is referred to in the literature as maximal-ratio-combining (MRC). The vector representation of the weighting factors for a X-element array is given by,

$$\mathbf{w} = [snir_1, snir_2, snir_3, ...snir_X]^T \tag{1.1}$$

The expression in Equation 1.1 relies heavily on the assumption that the channel is frequency-flat, and the interfering signals at each antenna element are statistically independent of one another [24]. In other words, the user signal experiences no delay spread, and the interfering signals impinging on each antenna element are unique. The MRC technique has been used in a wide range of mobile receiver applications due to its simplicity and ease of implementation, as well as significant performance gain [24]. The claim of optimality though, seems unreasonable due to the strict constraint imposed on the statistical properties of the interfering signals. In a mobile radio environment, it seem more reasonable to assume, that for a duration of time small compared to the fading rate ($I <<< f_d^{-1}$), both the desired and interfering signals impinging on the array are spatially correlated. By spatially correlated, it means that between antenna elements, signals exhibit some form of statistical similarity. With this in mind, given an array is made up of

a sufficient number of antenna elements, the output from each antenna should be able to be combined with other elements in the array in such a way as to both suppress co-channel interference, and simultaneously optimize the desired signal.

In [4] it was concluded, for a frequency-flat fading channel, a N-element array, can suppress up to N-2 interfering signals while at the same time provide diversity gain to the desired signal. To obtain this result the author used an antenna-combining scheme known in the literature as an optimum combiner (OC). The OC weights are given by the following expression,

$$\mathbf{w} = \alpha \mathbf{R}_{nn}^{-1} \mathbf{u}_d^* \,, \tag{1.2}$$

where $\mathbf{R}_{nn}$ is the statistical interference plus noise correlation matrix expressed by,

$$R_{nn} = E\{\mathbf{n}(nT)^* \mathbf{n}(nT)^T\}, \tag{1.3}$$

and $\mathbf{n}(nT)$ is a X-element vector whose elements are the interfering signals and noise at each antenna, and $\mathbf{u}_d$ is desired signals' propagation vector. As was mentioned above the expectation in Equation 1.3 should be taken over a period of time that is small compared to the fading rate.

As was the case with MRC, it can be proven that the OC maximizes the user's SNIR. Actually, if one were to assume no correlation between antenna elements, which is the model used to develop the MRC, it can be proven that the OC reduces to MRC. Therefore, in the context of a flat-fading channel, the OC is a generalized structure that maximizes the user's SNIR without the need of correlation that may or may not exist between antenna elements. In [4] the author showed that if one assumes correlation

between antenna elements, in the context of a frequency-flat fading channel with co-channel interference, the OC outperformed MRC for an IS136 digital mobile system. The result isn't surprising, since with the OC correlation that exists between antenna elements is utilized as seen by the use of the term $\mathbf{R}_{nn}$ in the expression for the OC weights in Equation 1.2.

As was mentioned previously, the need to combat multi-path propagation, in an effort to reduce the impact the error floor effect has on system performance, requires that some from of equalization be implemented as part of any digital mobile receiver design. To address the issue of multi-path the OC would have to be extended to include temporal processing. In [11,12] an OC receiver was proposed which included both spatial and temporal components. The structure consists of a bank of analog filters, a filter for each antenna, which are summed, sampled, than fed to a discrete, possibly infinite tap symbol spaced transversal filter.

The operation of this OC can be broken down into two basic steps. First, because the analog filter at each antenna is matched to the desired signal's channel response for that specific element, maximum SNR at the output of each filter is achieved. Next, the transversal filter, operating on the combined output from the bank of matched filters, neutralizes the multi-path by flatting the response at the output. More detail on this combiner is presented in Chapter 2 along with some performance results. The OC structure is shown below in Figure 1.3.

With regard to optimality, the only caveat here is that even though this structure minimizes the mean square error (MMSE) between the desired signal and the combiner

output, it does so only if one assumes the noise at the receiver to be temporally and spatially white, and the transversal filter of possibly infinite length.

If for example, one assumes co-channel interference, which is correlated between antenna elements when one develops the OC, the resultant structure would be very different. An extension of the OC for channels with correlated co-channel interference was proposed in [6] The design is just a generalization of the structure in [9] to provide for multiple antennas.

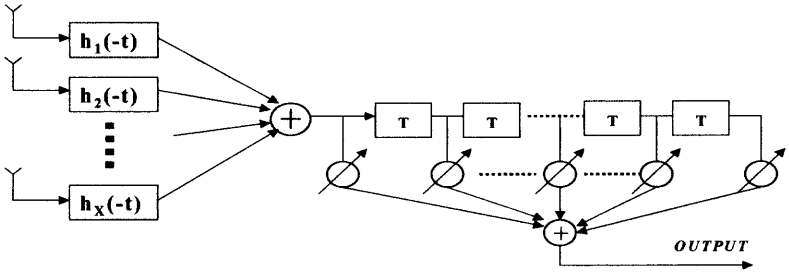

Figure 1.3 Optimum Combiner for signals with delay spread in AWGN.

Since in theory the bank of discrete filters that are used in this design may require an infinite number of taps to reach maximum performance, a relationship between the tap length and performance was developed [5]. The results show that for a two-path symbol spaced channel with one equal power interferer and an Eb/N_0 of 18 db fourteen causal taps and five non-causal taps are necessary.

A logical optimization criterion for any digital communications receiver is the minimization of the bit error rate (BER). Since BER is directly proportional to quality of service, a structure that yields a minimized BER can be used as a performance benchmark to compare against various other receivers. Even though some structures mentioned in the previous paragraphs did maximize the SNIR, few could claim to minimize the end-user's bit error rate (BER). For this reason, many authors have investigated the use of non-linear space-time processors in the hope of finding structures that achieve this goal. As was the case for linear space-time processors, the environmental impairments one assumes play a vital role in the resultant design of these non-linear structures.

1.2 Non-Linear Space-Time Processing

Many authors have investigated the development of structures that minimize the probability of error in the context of a single channel system, single channel meaning one transmitter and one receive antenna [3], [8]. In Chapter 3 it is shown, for a single channel system, given all possible signals are equal-likely and the random noise at the input of the channel can be statistically defined, a receiver designed to maximize the so-called likelihood function, will, at the same time minimizes the probability of sequence error. These structures are referred to in the literature as Maximum Likelihood Estimators (MLSE). Their derivation stems from a classic detection problem, in which one of N-possible signals embedded in noise is selected as the most likely to have been transmitted, based on the signal observed at the receiver and the statistical nature of the noise. It was

shown in [25] that by using this maximum likelihood decision rule the probability of a detection error is minimized.

One particular benefit in using the MLSE is it's passive nature, passive in the sense that the observed signal is left unmodified. This eliminates the possibility of noise enhancement due to deep nulls in the desired signal's channel response, which can be a problem for linear equalizers. The interest in the MLSE is due to its' superior performance over other methods, its' drawback is its' complexity. In recent years though, faster digital signal processors (DSP) with on-board MLSE units have become popular. This drastically reduces the complexity of implementation, making it easier than ever to integrate the MLSE into future receiver designs.

Array processing MLSE structures have been investigated by many authors. The largest body of work suggests incorporating the output from a bank of antennas into the calculations for the MLSE state transition metrics. In order to perform these calculations one needs to accurately describe the statistical properties of the noise at the input to the antenna array. This is a daunting task at best when interference is present. The difficulty comes from the non-stationary nature of the interference. As was the case for linear equalization there becomes a need to make some assumptions with regard to the nature of the interference.

In the present non-linear case, our interest is in the statistical properties of the interference in both the temporal and spatial domains. If one could accurately characterize these statistics, it is theoretically feasible that one could derive an array processing MLSE that provides optimum performance. To do this would require a very complex design, so,

instead, to reduce complexity most authors invoke the central limit theorem, inferring that the interference and noise process at the input to the array is Gaussian.

The most generalized statistical model assumes correlation exits in both the temporal and spatial domains [20]. In order to use the generalized model one needs to estimate, for a X-element array, a time dependent X by X dimensional correlation matrix, an a intimidating undertaking. Due to the complex nature of the estimator, most authors eliminate the time dependence by assuming the noise plus interference process is stationary and temporally white. This leads to a simpler design, which can be more easily implemented. The drawback here is that by simplifying the design in any way the claim of optimality is no longer valid. An additional simplification can be made by assuming the interference plus noise to be both spatially and temporally white. The result is a diagonal correlation matrix, and is likened to the linear method of MRC. In [19] the author shows that given certain environmental impairments the array processing MLSE can reduce to either the OC or MRC, both linear combing methods. Even with the simplification mentioned above, simulations have shown that the array processing MLSE performs as well or better than any of the linear-combing-methods. Of coarse the more complex the design the better the performance but simplified designs are easily implemented and the performance degradation may not be too substantial based on the actual statistical properties of the interference process.

1.3 Proposed Hybrid Method

A method is proposed which is similar in structure to the variety of array processing MLSE described previously, but that operates on the received signal in a very different manner. The design is referred to as the Canceller/MLSE. In our receiver, the array and MLSE work independently. They are linked by a common channel estimator, which is used by the MLSE for metric calculation, and by the antenna array for training the array weights. The motivation for separating the MLSE and antenna array is twofold.

First, to eliminate co-channel interference before the signal is applied to the sequence estimator, reduces the MLSE complexity, since the need for a complex estimate of the co-channel statistics would be unnecessary. To achieve this goal, the need is to focus the array on interference cancellation alone. This leads us to the second point for separating the array and MLSE. If the desired signal undergoes multi-path propagation, the array will attempt to equalize the signal by neutralizing any multi-path components present in the composite waveform. This limits the degree of freedom inherent in the array for interference cancellation. A method for training the array to avoid this degradation, has been proposed. To accomplish this by filtering, the locally generated training sequence is filtered through the channel estimator, than the modified sequence is used to train the array. This prevents the array from wasting any degrees of freedom for in-band interference cancellation on neutralizing multi-path from the desired signal. The dispersive desired signal should pass through the array unperturbed. Temporal equalization can then be handled by the MLSE and all degrees of freedom for signal suppression are preserved in canceller array.

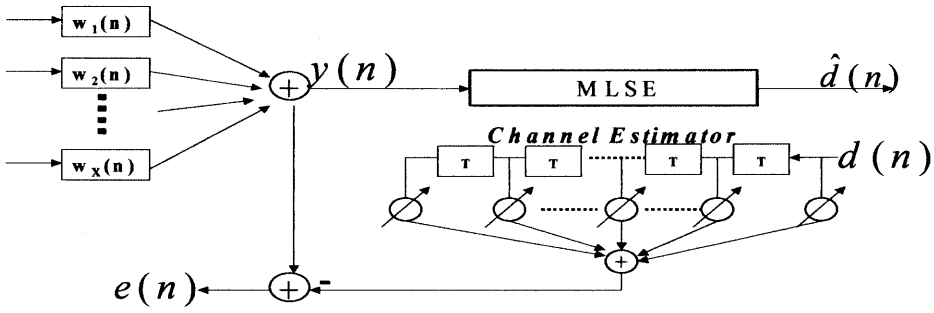

Figure 1.4 Proposed Canceller/MLSE design.

A diagram of the proposed design is shown in Figure 1.4. What is not clear from the figure is that the input to the canceller/mlse is actually the Ts-sampled output from a predefined receive filter. The receive filter has been designated by the IS136 standard which is the digital mobile system used for all the simulations in this thesis. To obtain the channel estimator weights and the array weights, joint optimization using the MMSE criteria is performed. This leads us to a result that requires constraints on the coefficients. Both linear and quadratic constraints on the channel estimator coefficients, have been investigated. The latter results in an eigen-value problem, which has been found through simulation, to produce the best performance.

In Chapter 4, the derivation of the Canceller/MLSE assuming frequency-flat faded co-channel interference. This model is used to prove the design can be optimal in the mean square sense. Two possible methods to improve the performance of the Canceller against dispersive interferers, have been investigated.

The first is the addition of antenna elements in the canceller array. Through simulation, it is shown that the additional antennas can adequately suppress dispersive interference, even when the multi-path components outnumber the antennas used in the array.

The second method is the addition of temporal taps at the input of each antenna element. An example of the proposed design is shown in Figure 1.3. The intention is to use these temporal taps for interference cancellation alone, leaving the desired signal's equalization to the MLSE. To achieve this goal, joint optimization of the array weights and estimator parameters is no longer considered. Instead, a two-step process is proposed. The channel estimator weights and center tap array coefficients are determined using the procedure developed for the flat-fading interference case. The results from the first step are used to determine the complete set of array coefficients. Simulations have proven this method to be an effective one, providing improvement over a canceller with no temporal taps. The method also outperforms a space-time array differential detector combination, with more temporal taps than the Canceller/MLSE.

The final method is simply an extension of the flat-faded interference case, but with the addition of temporal array taps. Results show that it is necessary to constrain the channel estimator coefficients to be causal when this method is used otherwise the performance is significantly degraded. However, simulation shows that this method outperforms the two-step procedure mentioned previously.

A comparison of the performance against interferers with delay spread between the two enhanced cancellers is performed, one with additional antennas, the other with

the addition of temporal array taps. It is found that the performance of the two are comparable given that enough temporal taps are added to the latter Canceller. Results are presented in Chapter 5.

CHAPTER 2

Spatial Processing Using Multiple Antennas

2.1 Antenna Combining Schemes

In narrow band communication channels where signal fading degrades the performance of receivers, antenna diversity is usually implemented. These co-located multiple antenna configurations not only provide diversity gain but also improve performance by suppressing co-channel interference. There are many techniques used for combining the signals from the receive antennas. The basic structure used for the majority of the linear combining methods is given by,

$$Y(t) = \sum_{x=1}^{X} w_x(t,\tau) * x_x(\tau), \tag{2.1}$$

where * denotes convolution, $x_x(\tau)$ is the observed signal at each of X antenna elements, $w_x(t,\tau)$ is a possibly time-varying weight function which needs to be determined based on the optimization criteria used, and $Y(t)$ is the optimized output. In vector format Equation 2.1 can be described by,

$$Y(t) = \mathbf{w}^T * \mathbf{x}, \tag{2.2}$$

where boldface denotes a vector and,

$$\mathbf{x}^T = [x_1(\tau), x_2(\tau), x_3(\tau), ..., x_X(\tau)]^T \text{ ,and } w^T = [w_1(t,\tau), w_2(t,\tau), w_3(t,\tau), ..., w_X(t,\tau)]^T.$$

Note that in Equation 2.1 the weights are functions of two variables. This is required since the weight functions generally need to be adapted over time to track the time variations in the mobile radio channel. The adaptation must be fast enough to track

these variations. Much work has been done on the performance of various tracking algorithms. In [2], results show that using the DMI algorithm a degradation of less than 0.2 dB can be expected due to tracking errors for speeds up to 60 mph. The focus of this thesis is the performance of antenna combining schemes in ideal conditions. *Therefore, in all the work presented here the channel is assumed static over the observation period. Hence, the dependence on time will be removed from Equation 2.1 leaving,*

$$. \; Y(t) = \sum_{x=1}^{X} w_x(\tau) * x_x(\tau) . \tag{2.3}$$

For mobile radio channels in which both desired and interfering channels are described as frequency flat there is no temporal correlation to utilize so the weight functions in Equation 2.3 need only take the form of multiplicative constants $w_x\delta(\tau)$, which are just weighted impulses. The Equation 2.3 then reduces to,

$$Y(t) = \sum_{x=1}^{X} w_x x_x(t) . \tag{2.4}$$

2.1.1 Combining Methods for User Signals with No Delay Spread in AWGN

Using Equation 2.4 now attempt to find a weight vector that will maximize some optimization criteria. A logical criteria would be maximizing the signal to noise ratio (SNR) at the output of the array. In [24] it was concluded that the maximum SNR at the output of the array could be obtained by weighting each signal by the SNR at the input to each antenna element and combining the result. This technique is referred to as maximal ratio combining (MRC) and the weights are given by ,

$$\mathbf{w} = \boldsymbol{\alpha}^{0H}, \tag{2.5}$$

where the *H* denotes a Hermitian Transpose and the noise term has been removed since it's assumed the same at each antenna element.

This is essentially a vector representation of a matched filter. The SNR at the output of the array then becomes,

$$SNR_{MRC} = \frac{\left|\sum_{x=1}^{X}\left|\alpha_x^0\right|^2\right|^2 \left|a^0(nT)\right|^2}{E\left\{\left|\sum_{x=1}^{X}\alpha_x^0 n_x(nT)\right|^2\right\}} = \frac{\left\|\boldsymbol{\alpha}^0\right\|^2}{\sigma_n} \quad . \tag{2.6}$$

Noting that for IS136 $\left|a^0(nT)\right|^2 = 1$.

From Equation 2.5, to implement MRC an accurate estimate of the desired signals channel vector, $\boldsymbol{\alpha}^0$ is needed. Errors in the estimate of these parameters will result in degradation of the combiners performance. To eliminate the need for the channel vector estimate, the signals can be combined (in all these derivations it's assumed that the signals at each antenna element have been phase aligned) from each of the antennas using weights with unity gain. The result is referred to as equal gain combining [24]. The output SNR is given as,

$$SNR_{EGC} = \frac{\left|\sum_{x=1}^{X}\alpha_x^0\right|^2 \left|a^0(nT)\right|^2}{E\left\{\left|\sum_{x=1}^{X} n(nT)_x\right|^2\right\}} = \frac{\left\|\boldsymbol{\alpha}^0\right\|^2 + \sum_{i=1}^{X}\sum_{\substack{j=1 \\ i\neq j}}^{X}\alpha_i^0\alpha_j^{0*}}{X\sigma_n} \quad . \tag{2.7}$$

A bound can be found on Equation 2.7 to better compare the SNR's for the combiners, by using the following inequality,

$$\sum_{i=1}^{X}\sum_{j=1}^{X}\left|\alpha_i^0-\alpha_j^0\right|^2\geq 0\,. \tag{2.8}$$

Expanding Equation 2.8 we get,

$$\sum_{i=1}^{X}\sum_{j=1}^{X}\{\left|\alpha_i^0\right|^2+\left|\alpha_i^0\right|^2-\alpha_i^0\alpha_j^{0*}-\alpha_i^{0*}\alpha_j^0\}\geq 0\,, \tag{2.9}$$

$$\sum_{i=1}^{X}\sum_{j=1}^{X}\{\left|\alpha_i^0\right|^2+\left|\alpha_i^0\right|^2\}-\sum_{j=1}^{X}\left|\alpha_j^0\right|^2-\sum_{i=1}^{X}\left|\alpha_i^0\right|^2-\sum_{i=1}^{X}\sum_{\substack{j=1\\ i\neq j}}^{X}\alpha_i^0\alpha_j^{0*}\geq\sum_{i=1}^{X}\sum_{\substack{j=1\\ i\neq j}}^{X}\alpha_i^{0*}\alpha_j^0\,. \tag{2.10}$$

Equation 2.10 reduces to,

$$(X-1)\sum_{j=1}^{X}\left|\alpha_j^0\right|^2-\sum_{i=1}^{X}\sum_{\substack{j=1\\ i\neq j}}^{X}\alpha_i^0\alpha_j^{0*}\geq\sum_{i=1}^{X}\sum_{\substack{j=1\\ i\neq j}}^{X}\alpha_i^{0*}\alpha_j^0\,. \tag{2.11}$$

Inserting Equation 2.11 into Equation 2.7 we get the inequality,

$$\frac{X\left\|\boldsymbol{\alpha}^0\right\|^2-\sum_{i=1}^{X}\sum_{\substack{j=1\\ i\neq j}}^{X}\alpha_i^0\alpha_j^{0*}}{X\sigma_n}\geq\frac{\left\|\boldsymbol{\alpha}^0\right\|^2+\sum_{i=1}^{X}\sum_{\substack{j=1\\ i\neq j}}^{X}\alpha_i^{0*}\alpha_j^0}{X\sigma_n}\,. \tag{2.12}$$

Where we have used $\sum_{j=1}^{X}\left|\alpha_j^0\right|^2=\left\|\boldsymbol{\alpha}^0\right\|^2$.

Therefore, we find

$$SNR_{MRC}-\frac{\sum_{i=1}^{X}\sum_{\substack{j=1\\ i\neq j}}^{X}\alpha_i^0\alpha_j^{0*}}{X\sigma_n^2}\geq SNR_{EGC}\,. \tag{2.13}$$

Equation 2.13 shows that MRC always has better performance than EGC.

The technique referred to as Optimum Combing combines the signals in such a way as to maximize the signal to noise SNR. The weights for the optimum combiner are calculated as [27, eq 2-41],

$$\mathbf{w} = \mu R_{I+n}^{-1} \boldsymbol{\alpha}^{0*} \quad , \tag{2.14}$$

where R_{I+n} is the interference plus noise correlation matrix (see Equation 2.17 for the definition of an autocorrelation matrix) and μ is a constant that has no effect on the overall SNR. For the case of no co-channel interference the expression in Equation 2.14 reduce to Equation 2.5. Therefore, the SNR is the same as for MRC.

Hence,
$$SNR_{OC} = \frac{\left\|\boldsymbol{\alpha}^{0}\right\|^2}{\sigma_n} \quad . \tag{2.15}$$

The last structure investigated is one that minimizes the mean square error between the observed signal and a locally generated replica of the desired signal. As is implied in the definition of the optimization criteria, this method requires that a training sequence be embedded in the user's data. In IS136, there is a fourteen-symbol block of data at the beginning of every data frame to accommodate this need. The weights for the MMSE combiner are given by [2],

$$\mathbf{w} = R_x^{-1} \mathbf{r}_{xd} \, , \tag{2.16}$$

where $\mathbf{r}_{xd}$ is cross correlation vector between the locally generated training symbol sequence "*d(nT)*" and the observed signal at each receive antenna and R_x is the observation correlation matrix given by,

$$R_x = E\left\{\mathbf{x}(nT)^* \mathbf{x}(nT)^T\right\} \, , \tag{2.17}$$

$$\mathbf{r}_{xd} = E\{\mathbf{x}^*(nT)d(nT)\}, \tag{2.18}$$

where x is a X-dimensional vector defined in Equation 2.2. The expressions in Equation 2.17 and Equation 2.18 can be approximated assuming an Z-symbol training sequence by,

$$\mathbf{r}_{xd} = \frac{1}{Z}\sum_{n=1}^{Z} x_x^*(nT)d\ (nT),\ x=1,2,3,...,X, \tag{2.19}$$

$$R_x(i,j) = \frac{1}{Z}\sum_{i=1}^{Z} x_j(nT)x_i^*(nT),\ \ i,j=1,2,3,4,....,X. \tag{2.20}$$

Applying Equation 2.17 for a flat-faded channel with no co-channel interference we get,

$$R_x = E\{(\boldsymbol{\alpha}^0 a^0(nT)+\mathbf{n})^*(\boldsymbol{\alpha}^0 a^0(nT)+\mathbf{n})^T\} = \boldsymbol{\alpha}^{0*}\boldsymbol{\alpha}^{0T} + \sigma_n I, \tag{2.21}$$

and,

$$\mathbf{r}_{xd} = E\{(\boldsymbol{\alpha}^0 a^0(nT)+\mathbf{n})^* a^0(nT)\} = \boldsymbol{\alpha}^{0*}. \tag{2.22}$$

Where the expectation has been taken with respect to the information symbols and the noise, assumed statistically independent of one another, and the magnitude of the symbols is assumed unity.

After some manipulation the expression in Equation 2.16 can be represented as [26, eq. 26],

$$\mathbf{w} = \frac{R_n^{-1}\boldsymbol{\alpha}^{0*}}{1+\boldsymbol{\alpha}^{0H}R_n^{-1}\boldsymbol{\alpha}^0}. \tag{2.23}$$

This is the same as Equation 2.14 except for a constant in the denominator.

From Equation 2.23 the SNR for the MMSE combiner for any channel is the same as OC, so,

$$SNR_{MMSE} = \frac{\mathbf{w}^H R_s \mathbf{w}}{\mathbf{w}^H R_n \mathbf{w}} = \frac{\left\|\boldsymbol{\alpha}^0\right\|^2}{\sigma_n} = SNR_{OC}, \tag{2.24}$$

where R_s is the desired signal's autocorrelation function.

Noting that from Equation 2.24 the performance of MMSE and OC are identical for channels with only AWGN.

By inspection of Equation 2.23, it can be seen that this is also the case for a channel with interference as well just by replacing R_n by R_{I+n}. The expression in Equation 2.16 is a much simpler form than in Equation 2.23 since there is no need to estimate the noise plus interference autocorrelation matrix, instead the correlation matrix of the observed data can be used.

A graph of results from a simulation of an IS136 system for all four structures is shown below. The simulation is for a frequency-flat fading channel with AWGN and no co-channel interference.

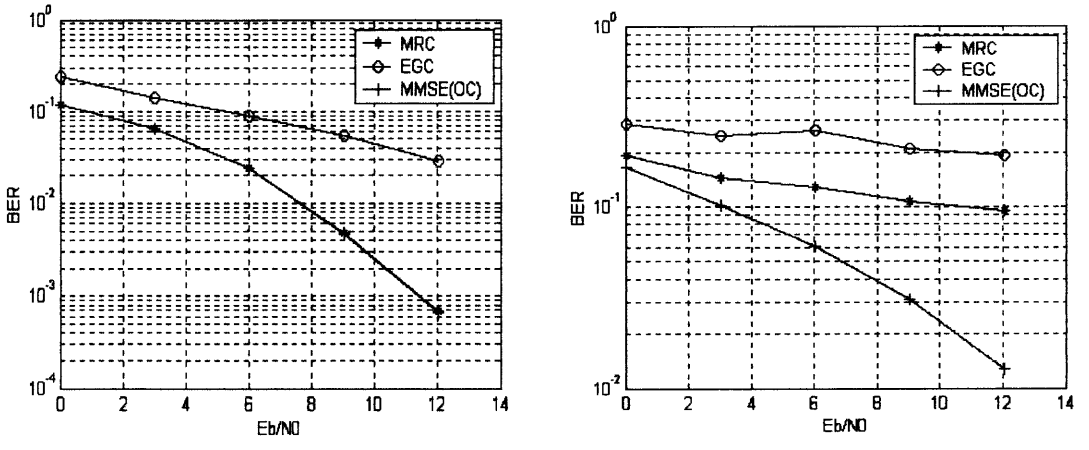

Figure 2.1 No co-channel interference (left) one equal power interferer (right), for an fd of 0 Hz.

In the study presented above, it is assumed no co-channel interference in the signal received at the mobile. One of the major benefits of combiners is their ability to suppress interference. The combiners that utilize information about co-channel interference, which might be present in the observed signal, have better performance in environments that include interference. In [4] a comparison between MRC and OC was performed. The results showed that OC outperformed MRC in all cases when interferers were present. This result makes sense if one notices that the MRC weights only include information about the desired signal, Equation 2.5), whereas OC, Equation 2.14), uses information about the desired signal, the noise and the interference when calculating the optimum weights.

The SINR for MRC combing is given by,

$$SINR_{MRC} = \frac{(\boldsymbol{\alpha}^{0H}\boldsymbol{\alpha}^{0}a^{0}(nT))^{H}(\boldsymbol{\alpha}^{0H}\boldsymbol{\alpha}^{0}a^{0}(nT))}{E\left\{(\boldsymbol{\alpha}^{0H}(\sum_{l=1}^{L}\boldsymbol{\alpha}^{l}I(nT)+\mathbf{n}))^{H}(\boldsymbol{\alpha}^{0H}(\sum_{l=1}^{L}\boldsymbol{\alpha}^{l}I(nT)+\mathbf{n}))\right\}}. \tag{2.25}$$

Where the expectation is done with respect to the data symbols and the noise. NOTE: The max fading rate is ~ 184 Hz and 1/184 is ~ 5000us in IS136 the symbol rate is 41.1us so it is assumed the averages here are over a large enough period to see the symbol statistics (~ 25 symbols) but small enough so that the fading is assumed constant.

Defining $\mathbf{x}_{I+n} = \sum_{l=1}^{L}\boldsymbol{\alpha}^{l}I(nT)+\mathbf{n}$ we get,

$$SINR_{MRC} = \frac{\left|\left\|\boldsymbol{\alpha}^{0}\right\|^{2}\right|^{2}}{E\left\{\left|\boldsymbol{\alpha}^{0H}\mathbf{x}_{I+n}\right|^{2}\right\}} = \frac{\left|\left\|\boldsymbol{\alpha}^{0}\right\|^{2}\right|^{2}}{\boldsymbol{\alpha}^{0T}R_{I+n}\boldsymbol{\alpha}^{0*}}. \tag{2.26}$$

Note that the SINR in Equation 2.26 is a random variable that varies at the fading rate [4] and the average over a period much longer than the fading rate is,

$$\mathbf{SINR}_{MRC} = E\{SINR_{MRC}\}. \tag{2.27}$$

Where notation, $\mathbf{SINR}_{MRC}$ is used, instead of $SINR_{MRC}$ to denote an average over the fading.

Since it is known from Equation 2.13 that MRC outperforms EGC the latter is not included in the analysis of SINR. Include is OC which has a SINR expression given as,

$$SINR_{OC} = \frac{(\mathbf{w}^{T}\mathbf{x}_{s})^{*}(\mathbf{w}^{T}\mathbf{x}_{s})^{T}}{E\left\{(\mathbf{w}^{T}\mathbf{x}_{I+n})^{*}(\mathbf{w}^{T}\mathbf{x}_{I+n})^{T}\right\}}. \tag{2.28}$$

Using Equation 2.14), Equation 2.26 becomes,

$$SINR_{OC} = \frac{\boldsymbol{\alpha}^{0T}R_{I+n}^{-1}R_{s}R_{I+n}^{-1}\boldsymbol{\alpha}^{0*}}{\boldsymbol{\alpha}^{0T}R_{I+n}^{-1}\boldsymbol{\alpha}^{0*}}. \tag{2.29}$$

Where $\mathbf{x}_{s}$ and $\mathbf{x}_{I+n}$ are the signal portion and interference plus noise portion of $\mathbf{x}$, respectively.

Using Equation 2.17 the expression in Equation 2.29 becomes,

$$SINR_{OC} = \frac{\boldsymbol{\alpha}^{0T}R_{I+n}^{-1}\boldsymbol{\alpha}^{0*}\boldsymbol{\alpha}^{0T}R_{I+n}^{-1}\boldsymbol{\alpha}^{0*}}{\boldsymbol{\alpha}^{0T}R_{I+n}^{-1}\boldsymbol{\alpha}^{0*}} = \boldsymbol{\alpha}^{0T}R_{I+n}^{-1}\boldsymbol{\alpha}^{0*}, \tag{2.30}$$

which is the same as the expression in [27, eq. 2-43].

Since a conditional expectation (short term statistics (i.e.: a period much less than the fading rate)) has been used in all the previous results the channel coefficients have

remained fixed. Long-term statistics would take into account the statistical nature of the channel coefficients. In all the work done for this thesis, the channel coefficients are assumed zero mean complex Gauss Ian processes with non-flat power spectral densities. The expressions in Equation 2.29 and Equation 2.26 have been analyzed for one or two interfering signals in [4] and for multiple interferers in [22]. Below is a graph of the ratio of the SINR for OC and MRC, which have been derived using Monte Carlo simulations.

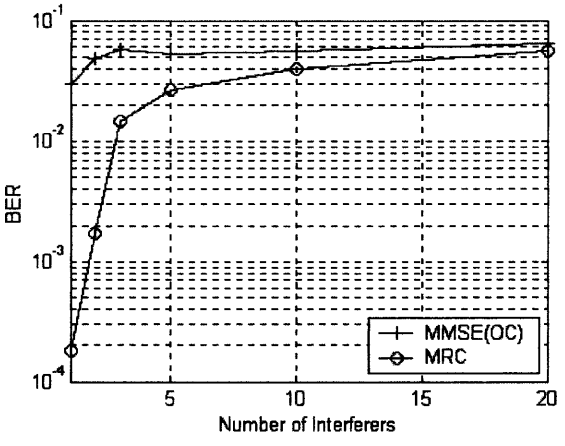

Figure 2.2 Performance of three antenna combiners, Eb/N_0=17 db, C/I=3 db.

In most mobile radio environments, both the desired and interfering signals are subject to dispersion in the time domain because of multi-path propagation. In order for reliable communication to occur in this environment, the mobile receiver must be equipped with a means to compensate. Temporal equalizers have been shown to provide a significant improvement in receiver performance by removing distortion from the desired signal. The methods are either linear as is the case with FIR filtering or non-linear, examples of which are decision feedback (DFE), and maximum likelihood estimation. Maximum likelihood estimation, unlike the other two methods is passive in the sense that

the received signal is not modified and then sent on to a slicer. Instead, the observed signal is discarded after being used to estimate the desired data. This is a benefit since other methods can enhance the noise at the input to the receiver while trying to equalize the desired signal. Multi-path rays incident on the receive antenna cause temporal distortion of the received signals as mentioned above, but they also possess spatial characteristics which can be exploited to remove them. Similar to the way the combiners remove co-channel interference additional antennas can also be used to remove the temporal distortion caused by the delayed multi-path rays. The method of using additional antennas follows the same logic as described above for co-channel interference except that each of the delayed rays is treated as an interferer that must be removed by the combiner. This scenario was analyzed in the previous section. Here, the concept of joint spatial-temporal equalization using what is referred to as space-time structures, since they work on the receive signal in both the spatial and temporal domains, is introduced, by first investigating the linear filtering method proposed in [11] for a channel with time dispersion, but no co-channel interference. First, it's necessary to define an upper bound on the performance of a multi-antenna configuration that can be used as a benchmark when comparing various techniques.

2.1.2 Matched Filter Bound

The matched filter bound is the performance of a combiner with summed front-end Matched filters subject to a flat-faded channel. The expression for the matched Filter bound is given by [11, eq 20],

$$P_{emf} \leq \exp\left\{-\frac{1}{N_0}\sum_{x=1}^{X}\int_{-\infty}^{\infty}|f_x(t)|^2\right\}. \tag{2.31}$$

2.1.3 Combining Methods for User Signals with Delay Spread in AWGN

2.1.3.1 Linear Methods. Many papers were written which covered the topic of optimum filtering for an infinite sequence of pulses subject to a dispersive channel and AWGN. In [7] the author derived a structure for maximizing the SNR at the output of the filter. He included the desired signal's ISI terms in the overall expression for the noise introduced by the channel. His result was a receive filter composed of two parts. The first part is an analog filter matched to the impulse response of the convolution of the transmit filter and the channel's response. An infinite tapped delay line with tap spacing equal to the symbol period follows this. The tap coefficients are related to autocorrelation function of the overall channel response by,

$$\frac{N_0}{N_0 + \Phi^*(w)} = \sum_n f_n e^{-jwnT}. \tag{2.32}$$

Where N_0 is the noise energy, $\Phi^*(w)$ is the Fourier transform of the sampled autocorrelation function of the overall response of the channel, and f_n are the tap coefficients. From Equation 2.32 one can see that by including the noise energy in the calculation for the tap coefficients the noise enhancement problems that equalizers such as the zero forcing equalizer face are greatly reduced. In fact if the noise is the dominate term in the LHS of Equation 2.32 the f_n's are all zero except for n=0. Mathematically the tap delay line filter response would be f_n= δ(n), which would eliminate noise enhancement by the filter. The overall filter has the effect of first maximizing the signal

to AWGN ratio by using a front end filter matched to the channel response, then it eliminates the ISI by using an infinite length tapped delay line filter.

The method described in [11] is essentially an extension of the result obtained in [7] to channels with multiple receive antennas. The goal in this work was to find a structure that provided diversity reception and a means of mitigating the effects of inter-symbol interference. What they found was an optimum receiver which consisted of a bank of matched filters each matched to it's respective channel whose outputs are first summed than passed through a infinite length tapped delay line to remove ISI from the desired signal.

The tap coefficients are given by the following expression,

$$\frac{1}{\sum_{x=1}^{X} R_x(w) + \frac{N_0}{\sigma_c^2}} = \sum_n f_n e^{jnwT} \quad . \tag{2.33}$$

Where for IS136 σ_c^2=1 and,

$$R_x(w) = \frac{1}{T}\sum_l \left| F_x(w - \frac{2\pi l}{T}) \right|^2 , \tag{2.34}$$

and $F_x(w)$ is the Fourier transform of the overall sampled channel response, defined as the convolution of the transmit filter with the receive filter and the impulse response of the channel. The expression in Equation 2.32 is essentially a special case of the expression in Equation 2.33 with X=1 (one antenna case) and the addition of a noise term in the numerator. Of course it has been assumed that each of the antennas is time synchronized otherwise the tapped delay line concept would not be appropriate. The

criteria the authors use in [11] to determine this structure is the minimization of the mean square error defined as,

$$Min_{w_1(t),w_2(t),\ldots w_X(t)} E\left\{\left|V_o(0)-a_0\right|^2\right\}. \tag{2.35}$$

Where $V_o(0)$ is the sampled output from the sum of X filters each at the output of one of X antenna elements, and a_0 is the transmitted symbol at time instant *t=0*. There is no claim of optimality other than the minimum of the MSE, but it was shown that for rectangular constellations, the probability of error could be upper-bounded by [11 eq 19],

$$P_e \le \exp\left\{-\frac{(1-\frac{MSE}{\sigma_a^2})}{MSE}\right\}. \tag{2.36}$$

From the results in [11], it's seen that for a two path Rayleigh fading channel with inter-ray delay of T_s, the performance of this combiner/equalizer is within approximately three db of the matched filter bound for a BER of 10^{-4}.

From Equation 2.33 and Equation 2.34 one can see that this filter is essentially a zero forcing filter with the addition of the noise terms to reduce the possibility of noise enhancement if the overall channel response has deep nulls.

It's interesting to note that in Equation 2.33 when the channel response is flat and the combination of transmit and receive filters is Nyquist that $R_x(w)$ is a constant and the tap delay line response is $f_n = \beta\delta(n)$, which essentially indicates that there is no ISI to be removed from the desired signal. Also in this case, since the output from each matched filter is equal to the energy in the desired signal, and since matched filtering results in

phase equalization the summed output from the bank of matched filters closely approximates MRC, which is optimal for this type of scenario. From the discussion above one can see how this structure attains the goals the authors were trying to achieve of both diversity gain and removal of ISI from the desired signal.

In the paper mentioned above, the authors also touch on DFE structures but these will not be covered in this thesis. The DFE's performance is usually better than LE but suffer from error propagation where a symbol detected incorrectly can greatly reduce performance if the feedback filter has a considerably long length. This is because the error must propagate through the entire feedback path that affect the detection of succeeding symbols. In effect, one detection error can result in a possibility of many more errors since the detection of each succeeding symbol is dependent on the accuracy of the previous detected symbols through the feedback filter.

2.1.3.2 Non-Linear Methods. To begin with there must be an assumption made with regard to the statistical properties of the noise process in both the spatial and temporal domains. For the following structures, it has been assumed that the noise processes at each of the antennas is AWGN and statistically independent from one another. This means that the noise is statistically independent in both the spatial and temporal domains.

Given that the noise at the input to the N-antennas is a temporally white Gaussian random vector distributed by,

$$\mathbf{n} \sim N(\mathbf{0}, \boldsymbol{\sigma}_n), \tag{2.37}$$

the likelihood function can be written as [3, eq. 9][19, eq. 7],

$$L \sim \int_I \mathbf{n}^H(t) R_{nn}^{-1} \mathbf{n}(t) dt \sim \int_I \mathbf{n}^H(t) \mathbf{n}(t) dt, \tag{2.38}$$

where I is the interval over which the signal is observed.

The expression in Equation 2.38 can be expanded to give [3, eq. 8],

$$L \sim \int_I (\mathbf{y}(t) - \sum_{nT \in I} a_n \mathbf{h}(t - nT))^H (\mathbf{y}(t) - \sum_{nT \in I} a_n \mathbf{h}(t - nT)) dt, \tag{2.39}$$

where y is the observed signal vector whose elements are the observed signal at each of the antennas and **h** is the channel response vector whose elements are the channel response from the transmitter to each antenna. To find the most likely signal the symbol sequence {a} that maximizes the expression in Equation 2.39 must be found. To do this, first Equation 2.39 must be expanded, then simplified to yield [3, eq.11],

$$L \sim \sum_{nT \in I} 2\,\mathrm{Re}(a_n^* z_n) - \sum_{iT \in I} \sum_{kT \in I} a_i^* s_{i-k} a_k, \tag{2.40}$$

where,

$$z_n = \sum_{x=1}^{N} \int h_x^*(t - nT) y_x(t) dt, \tag{2.41}$$

$$s_l = \sum_{x=1}^{N} \int h_x^*(t - iT) h_x(t - kT) dt \qquad l = k - i, \tag{2.42}$$

and N is the number of antennas.

The expression in Equation 2.41 is in the same form as a matched filter. Therefore z_n can be thought of as the sampled summation of outputs from N-matched filters, such that the filter at the x^{th} antenna is matched to the channel response between the transmitter and the x^{th} antenna. The expression in Equation 2.42 is the sum of the convolution of each channel response with itself sampled at time instant lT. As can be

seen from these expressions, just as in the case of the linear equalizer the channel response must be estimated. Therefore, both structures suffer degradation in performance when there are estimation errors in estimating the channel response.

The maximization shown above can be performed iteratively using the Viterbi algorithm. The algorithm makes the computation linear in time, so that it's feasible to implement in a real application. Performance analysis for the MLSE is difficult to obtain, but with some reasonable assumptions, it was shown in [3, eq's. 48,49] that the MLSE receiver for QAM modulation has a lower BER than the infinite tap linear equalizer. Using [3, eq's 24,48,49] the expression for the performance gain can be written as,

$$10\log\left(T^2 \int_0^{1/T} S^*(f)df \int_0^{1/T} 1/S^*(f)df\right)(db), \tag{2.43}$$

where $S\ (f)$ is the Fourier transform of the channel response and T is the symbol period.

2.1.4 Combining Methods for User Signals with Delay Spread and Co-channel Interference in AWGN

2.1.4.1 Linear Methods. Up to this point, all the receiver structures were optimized assuming AWGN as the only impairment to reliable reception of the end-users information signal. Due to the limitations of spectrum allocation imposed on wireless service providers base stations which share the same user channel are usually within close enough proximity to one another that co-channel interference becomes a major part in the degradation of the mobile users' quality of service. Therefore, it becomes necessary to optimize receivers taking into account the interference from co-channel users. In [11] the optimum linear receiver was developed assuming only AWGN on the channel, the same concept can be expanded to include dispersive co-channel interference [5].

Using the same derivation described in [12], the optimum single antenna linear filter assuming a dispersive user channel with co-channel interference can be expressed as [10],

$$r_0(t) = \sum_{n=-\infty}^{\infty} a_{n0}\varphi_0^*(nT-t) + \sum_{i=1}^{L}\sum_{n=-\infty}^{\infty} a_{ni}\varphi_i^*(nT-t)\ , \tag{2.44}$$

where, $\varphi_i(t)$ is the channel response of the ith co-channel interferer and $\varphi_0(t)$ is the desired signal's response. The expression in Equation 2.44 shows that the optimum MMSE linear filter can be interpreted as a bank of filters at each antenna element matched to each of the L+1 arriving signals with a T-spaced infinite tapped delay line whose tap coefficients are given by a_{ni} following each matched filter. The outputs from each transversal filter are summed to form the optimum filtered output. As can be seen in Equation (2.44 the optimum filter now takes the co-channel interference into account as well as the noise. The noise component in the filter has been included in the expression for the taped delay line coefficients given as,

$$a_{ni} = \left\{ \begin{array}{l} -\frac{1}{N_0}u_{n0}.....i=0; n<0 \\ \frac{1}{N_0}(1-u_{00}).....i=0; n=0 \\ -\frac{1}{N_0}u_{ni}.....i=1,2,3,...,L; \forall n \end{array} \right\}, \tag{2.45}$$

$$u_{ni} = \int_{-\Re}^{\infty} \phi_i(nT-t)r_0(t)dt.$$

In [6], the problem was expanded to include a X-element antenna array. The expression for the optimum vector filter is given by,

$$\mathbf{f}_0(t) = \frac{1}{\widetilde{N}}\left\{\mathbf{h}_0^*(-t) - \sum_{l=0}^{L}\sum_{k=-\infty}^{\infty} a_l[k]\mathbf{h}_l^*(kT-t)\right\}, \tag{2.46}$$

where, $\mathbf{h}_0(t) = [h_0^1(t), h_0^2(t), h_0^3(t), ..., h_0^X(t),]^T$ is a vector whose elements are the channel response between the desired user's transmitter and each antenna element. The vector $\mathbf{f}_0(t) = [f_0^1(t), f_0^2(t), f_0^3(t), ..., f_0^X(t),]^T$ has elements, which are the optimum filters for each of the X antennas. The output from each of the antenna filters is then summed to form the final output. As was the case in Equation 2.44 the optimum vector filter takes into account both the noise and the co-channel interference. In this case, the correlation in both the time and spatial domain is utilized unlike Equation 2.44 where only the correlation in the time domain was utilized since only one antenna was used.

Since it's difficult to obtain an expression for the SNR, the MSE is usually used as a measure of the performance for these receiver designs. The expression for the MSE is given by [6],

$$MSE_{OC} = \frac{\sigma_s^2}{2\pi}\int_{-\pi}^{\pi}\frac{1}{r(w)+1}dw. \tag{2.47}$$

For the IS136 case, the BER was obtained through simulation and is shown in the figures below.

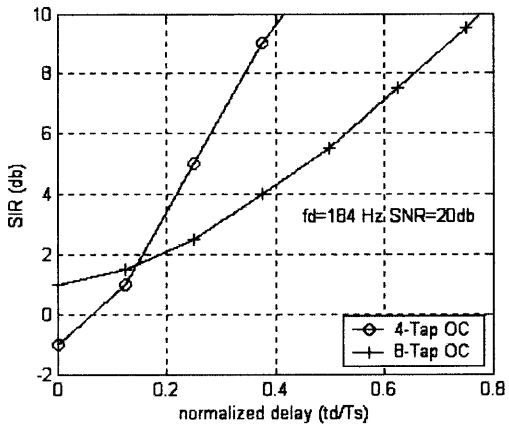

Figure 2.3 Performance of OC for constant BER of 10^{-2}.

2.1.4.2 Non-Linear Methods. The final topic of this section is the extension of the method shown in section 2.1.3.2 for the case where there is co-channel interference. For this case, it is necessary to take into account correlation between signals in both the spatial and time domains. The formulation becomes very cumbersome and is usually not used in practical applications because of this. Instead, it is usually assumed that the interference and noise on each of the X-channels can be modeled as stationary and white. Of course, this is not the case especially when there are few interferers present but the assumption has been shown to provide very good performance in simulation results. However, for completeness the derivation of a structure making no assumptions of this kind has been included following the derivation of [20] and assumming that each interference signal $v_i(t)$ can be modeled as a white Gaussian noise source with unity variance. This eliminates the rapid cyclostationary variation of the interference [20]. The interference signal passes through a transmit filter followed by the channel impulse response before impinging on the mobile's antenna array. The input to the array can be written as,

$$\mathbf{Int}_l(t) = \int_I v_l(t-\tau)\mathbf{g}_l(\tau)d\tau \quad , \tag{2.48}$$

where $\mathbf{g}_l(\tau)$ is the composite response of the transmit filter and vector channel response. The time domain autocorrelation function for the interference process can be expressed as,

$$R_{Int,Int}(t_1,t_2) = E\left\{\sum_L \mathbf{Int}_l(t_1)\mathbf{Int}_l^*(t_2)\right\} = E\left\{\sum_L \iint_I v_l(t_1-\xi)v_l(t_2-\psi)\mathbf{g}_l(\xi)\mathbf{g}_l^*(\psi)d\xi d\psi\right\} , \tag{2.49}$$

$$R_{Int,Int}(t_1,t_2) = \sum_L \int_I \mathbf{g}_l(\xi)\mathbf{g}_l^*(t_1-t_2-\xi)d\xi \quad . \tag{2.50}$$

The expression for the interference plus AWGN correlation matrix can now be written as,

$$R_{ww}(t_1,t_2) = \sigma_n^2\mathbf{I} + R_{Int,Int}(t_1,t_2) , \tag{2.51}$$

and the generalized expression for Equation 2.39 for channels with co-channel interference can be given as,

$$L \sim \int_I \int_I \mathbf{w}^H(t_1)R_{ww}^{-1}(t_1,t_2)\mathbf{w}(t_2)dt_1dt_2 , \tag{2.52}$$

The final expression now becomes,

$$L \sim \int_I \int_I (\mathbf{y}(t_1) - \sum_{nT\in I} a_n\mathbf{h}(t_1-nT))^H(t_1)R_{ww}^{-1}(t_1,t_2)(\mathbf{y}(t_2) - \sum_{nT\in I} a_n\mathbf{h}(t_2-nT))dt_1dt_2 , \tag{2.53}$$

which reduces to the same expression as Equation 2.40), repeated here as,

$$L \sim \sum_{nT\in I} 2\,\mathrm{Re}\left(a_n^* z_n\right) - \sum_{iT\in I}\sum_{kT\in I} a_i^* s_{i-k} a_k \quad ; \tag{2.54}$$

hence, with the proper definition of the parameters given by,

$$z_n = \iint_I \mathbf{h}(t_1 - nT)^H R_{ww}^{-1}(t_1,t_2)\mathbf{y}(t_1 - nT)dt_1 dt_2,$$
$$s_{l,n} = \iint_I \mathbf{h}(t_1 - nT)^H R_{ww}^{-1}(t_1,t_2)\mathbf{h}(t_1 - lT)dt_1 dt_2. \quad (2.55)$$

From Equation 2.55), it can be seen that to obtain the parameters necessary for the metric calculation, an estimate, not only of the vector channel response for the desired user $\mathbf{h}(t)$, but also the inverse of the interference plus noise time domain correlation function $R_{ww}^{-1}(t_1,t_2)$ is necessary. Where $R_{ww}^{-1}(t_1,t_2)$ is defined as,

$$\int_I R_{ww}^{-1}(t_1,t_2)R_{ww}(t_2,t_3)dt_2 = \mathbf{I}\delta(t_1 - t_3). \quad (2.56)$$

The accurate estimation of these parameters is essential for optimum performance of the MLSE. Possible inaccuracies in estimating metric parameters along with substantially increased complexity make this design impractical for real applications. The performance of a two-antenna configuration is shown below [20].

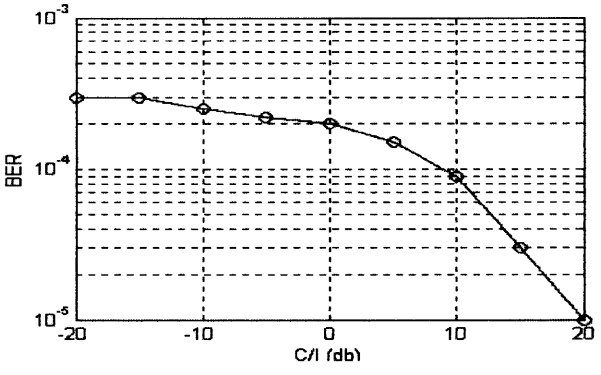

Figure 2.4 Performance for non-dispersive user signal, and one interferer, Eb/N_0=30 db.

CHAPTER 3

MAXIMUM-LIKELIHOOD SEQUENCE ESTIMATION

In the following, a structure is derived that is optimal for minimizing the probability of sequence error. This non-linear structure uses information about the channel to determine all possible data sequences that could be transmitted. The sequence that comes closest in signal space to the observed noisy signal is selected as the most likely sequence. It will be shown that finding the most likely sequence minimizes the probability of the sequence being in error.

If the transmitted symbols take on one of M possibly complex values, and the received block of data is N symbols in length, than there are a total of $M^{\wedge N}$ possible sequences which could have been sent by the transmitter. The issue is which of the $M^{\wedge N}$ possible sequences is the most likely one. To find it, the entire block of observed noisy signal samples will be needed. It will be shown in the proceeding sections, that these samples along with knowledge of both the channel impulse response, and the statistical nature of the noise, are enough information for determining, with minimum probability of error, which of the $M^{\wedge N}$ possible sequences was transmitted. In the following derivation, it's assumed the noise at the input to the receiver is white and Gaussian with zero mean and an unknown variance σ. Before the derivation can begin, it will be necessary to introduce the concepts of a signal-space and sufficient statistics. This will follow below.

3.1 Signal Space Representation of Signals

Briefly any determinate, finite-energy signal can be represented, over a specific time interval, by a series expansion of orthonormal bases functions of the form,

$$Y(t) = \sum_{n=1}^{n=K} \alpha_n \phi_n(t) \qquad t \in \{0,T\} \qquad K=1,2,3...,\infty, \tag{3.1}$$

where,

$$\alpha_n = 1/T \int_0^T Y(t)\phi_n(t)dt \tag{3.2}$$

The representation is in the sense that the mean square error between the LHS and the RHS of the Equation is minimized for a given value of K. Signal space is defined as a *K*-dimensional vector of the possibly complex values given by the weighting terms in the expansion. The signal space representation for the signal in Equation 3.1 has the form,

$$\mathbf{Y} = \boldsymbol{\alpha}^T , \tag{3.3}$$

$$\boldsymbol{\alpha} = [\alpha_1, \alpha_2, \alpha_3, ..., \alpha_K]. \tag{3.4}$$

3.2 Sufficient Statistics

If the mean square error between the LHS and RHS of Equation 3.1 approaches zero as the value for K is increased, the set of orthonormal functions is said to be complete for that signal. The signal is fully represented by the sum of expansion terms. The functions have been assumed to be complete for all the signals studied in this thesis. Given that the orthonormal functions in the expansion are deterministic, when the signal is statistical in nature, the coefficients in the expansion contain all the statistical information to describe

the signal. The vector of coefficients in Equation 3.4 form a set of sufficient statistics for the signal that can be used to identity it.

3.3 Derivation of MLSE Receiver

To begin, assume that the mobile receives over a time period $t \in \{0,T\}$ (T is assumed to be longer than the period required to receive the complete sequence) the summation of the transmitted signal and additive white Gaussian noise (AWGN). From the discussion of signal space and sufficient statistics, the signal received by the mobile can be described as an expansion, of the form given in Equation 3.1. Because the additive noise is white its' expansion will require an infinite number of terms. It's reasonable to assume that only a finite number of terms (K is used to describe the number of terms) is needed for a complete expansion of all the M^N possible transmitted signals. The obvious question is how many terms will be needed for the correct detection of one out of M^N possible signals, embedded in AWGN that could have been sent by the transmitter.

First, note that of the infinite number of expansion terms required to describe the signal at the mobile, only the first K statistics contain a desired signal component. If it can be proven that the remaining statistics are independent of the first K we can eliminate them since they add no additional information to the decision making process. To prove statistical independence,

$$E\{r_j n_i\} = 0 \ , \ j=1,2,3,....K, \quad i=K+1,K+2,..... \infty, \tag{3.5}$$

where r_j and n_i are the projection of the received signal and noise "r" and "n"onto the j^{th} and i^{th} dimension respectively of the signal space given by Equation 3.2 and E{.} is the expectation operator. The r_j in Equation 3.5 can be expanded as,

$$r_j = s_j^m + n_j \ , \qquad m=1,2,3,....M\text{^}N, \qquad (3.6)$$

than Equation 3.5 becomes,

$$E\{(s_j^m + n_j)n_i\} . \qquad (3.7)$$

Expanding Equation 3.7 we get,

$$\iint E\{[s^m(v)n(u)+n(u)n(v)]\Phi i(u)\Phi j(v)dudv\}, j=1,2,3,....K, \quad i=K+1,K+2,..... \infty,$$

(3.9)

"I" is the period in time the signal is observed.

Since the noise is assumed zero-mean and white Equation 3.9 reduces to,

$$\iint_I \sigma\delta(u-v)\Phi i(u)\Phi j(v)dudv \ , j=1,2,3,....K, \quad i=K+1,K+2,..... \infty. \qquad (3.10)$$

Since i never equals j, Equation 3.10 is always equal to zero, and the proof is complete. It can be concluded that all the information necessary for the detection of the desired signal is contained in the output of K correlators, of the form,

$$\int_I r(t)\Phi i(t)dt \ , \qquad i=1,2,3,....,K . \qquad (3.11)$$

The original analog detection problem has essentially been transformed into a discrete one (discrete in the sense that the indexes are not of time but signal dimension), for which a detection rule must be found.

An optimum detection rule should define decision regions in K-dimensional signal space such that the probability of selecting the wrong sequence is minimized. Mathematically, we will select $s^m(t)$ if,

$$\mathbf{r} \in \Theta_m, \quad m=1,2,....M^N, \tag{3.12}$$

where Θ_m is the decision region in K-dimensional signal-space for the signal.

To determine these decision regions first it is necessary to characterize the distribution of a K–dimensional random vector whose elements are the outputs from each of the correlators. Noting that the correlators in Equation 3.11 are linear, the noise at the output of each will be Gaussian with variance σ_n and mean equal to the projection of the transmitted signal onto that specific basis function. The set of K outputs forms the vector,

$$\mathbf{r} = \mathbf{s}^m + \mathbf{n} \tag{3.13}$$

$$\mathbf{s}^m = [s_1^m, s_2^m, s_3^m, ..., s_K^m]^T, \quad \mathbf{n} = [n_1, n_2, n_3, ..., n_K,]^T \qquad m=1,2,...,M^N$$

where the boldface denotes a vector.

Due to the orthomorallity of each of the basis functions, the noise at the output of each correlator will be uncorrelated. Therefore, it's correct to write the joint density function of the K-dimensional Gaussian vector conditioned on a particular signal transmitted as,

$$P(\mathbf{r}/\mathbf{s}^m) = \frac{1}{(2\Pi\sigma)^{K/2}} \exp\left[-\frac{1}{2\sigma^2}|\mathbf{r}-\mathbf{s}^m|^2\right]. \tag{3.14}$$

Since there are M^N possible sequences which can be transmitted there will be M^N possible distributions that the observed vector could have been drawn from and hence M^N decision regions to determine. First, it's necessary to determine an expression for the

probability for making a wrong decision. To do this, start by finding the probability of making a correct decision.

The probability of a correct decision can be written as,

$$P(correct) = \sum_{m} P(correct/\mathbf{s}^m)\,P(\mathbf{s}^m), \tag{3.15}$$

the probability of an error occurring is then $1 - P(correct)$, or

$$P(error) = 1 - \sum_{m} P(correct/\mathbf{s}^m)\,P(\mathbf{s}^m). \tag{3.16}$$

But the probability of a correct decision given signal "*m*" was sent is just,

$$P(correct/\mathbf{s}^m) = \iiint_{\Theta m} \ldots \int P(\mathbf{r}/\mathbf{s}^m)\,d\mathbf{r}, \tag{3.17}$$

so Equation 3.16 becomes,

$$P(error) = 1 - \sum_{m} P(\mathbf{s}^m) \iiint_{\Theta m} \ldots \int P(\mathbf{r}/\mathbf{s}^m)\,d\mathbf{r}. \tag{3.18}$$

Minimizing Equation 3.18 can be accomplished by selecting the decision regions Θ_m such that $P(\mathbf{s}^m)P(\mathbf{r}/\mathbf{s}^m)$ is maximum within the region.

The regions can then be selected by the following rule

$$\mathbf{r} \in \Theta_m \text{ if } P(\mathbf{s}^m)P(\mathbf{r}/\mathbf{s}^m) = \underset{i}{Max}\{P(\mathbf{s}^i)P(\mathbf{r}/\mathbf{s}^i)\}. \tag{3.19}$$

If signals are assumed to be equal likely, than Equation 3.19 becomes,

$$\mathbf{r} \in \Theta_m \text{ if } P(\mathbf{r}/\mathbf{s}^m) = \underset{i}{Max}\{P(\mathbf{r}/\mathbf{s}^i)\}, \tag{3.20}$$

and the maximum likelihood receiver rule can be described.

If $P(\mathbf{r}/\mathbf{S_m}) = \underset{i}{Max}\{P(\mathbf{r}/\mathbf{S}_i)\}$ then $\mathbf{S_m}$ was the most likely signal sent.

Plugging Equation 3.14 into Equation 3.20 we select the signal that maximizes,

$$\underset{i}{Max}\left(\frac{1}{(2\Pi\sigma)^{K/2}}\exp\left[\frac{-1}{2\sigma^2}\left|\mathbf{r}-\mathbf{s}^i\right|^2\right]\right). \tag{3.21}$$

To simplify the calculation the natural logarithm of Equation 3.21 can be used since the natural logarithm is a monotonically increasing function and we get,

$$\underset{i}{Max}\left(\left[\frac{-1}{2\sigma^2}\left|\mathbf{r}-\mathbf{s}^i\right|^2\right]+C\right). \tag{3.22}$$

The constants can be discarded since they don't affect the maximization. The result is,

$$\underset{i}{Max}\left(-\left[\left|\mathbf{r}-\mathbf{s}^i\right|^2\right]\right). \tag{3.23}$$

The expression in Equation 3.23), sometimes referred to as the minimum distance rule, can be expanded,

$$\underset{i}{Max}\left\{-|\mathbf{r}|^2+2\,\mathrm{Re}\left(\mathbf{s}^{iH}\mathbf{r}\right)-\left|\mathbf{s}^i\right|^2\right\}. \tag{3.24}$$

Since the power term is common to all hypotheses, the observed power term in Equation 3.24 can be omitted from the final expression. Finally, we have,

$$\underset{i}{Max}\left\{2\,\mathrm{Re}\left(\mathbf{s}^{iH}\mathbf{r}\right)-\left|\mathbf{s}^i\right|^2\right\}. \tag{3.26}$$

The rule in Equation 3.26 can be related to the original problem by using the relationships in Equation 3.1 and, Equation 3.2 and the orthomormality of the bases functions,

$$\int_I \sum_n \sum_m s_n^{i*} r_m \Phi_n(t)\Phi_m(t)dt = \int_I s^i(t)^* R(t)dt\ , \tag{3.27}$$

$$\int_I \sum_n \sum_m s_n^{i*} s_n^i \Phi_n(t)\Phi_m(t)dt = \int_I s^i(t)^* s^i(t)dt\ . \tag{3.28}$$

The expression in Equation 3.28 now becomes,

$$\underset{i}{Max}\left\{2\,\mathrm{Re}\left(\int_I s^i(t)^* R(t)dt - \frac{1}{2}\int_I s^i(t)^* s^i(t)dt\right)\right\}. \tag{3.29}$$

A receiver, as the one described by Equation 3.29 is impractical for large sequences since there are M^N possible signals hence M^N correlators are needed. To reduce this number to only one, expanding Equation 3.29 we get,

$$\underset{i}{Max}\left\{2\,\mathrm{Re}\left(\int_I \sum_n a_n^{i\,*} h(t-nT)^* R(t)dt - \frac{1}{2}\int_I \sum_n \sum_m a_n^{i\,*} a_m^i h(t-nT)^* h(t-mT)dt\right)\right\},$$

(3.30)

which can be simplified to give,

$$\underset{i}{Max}\left\{2\ \mathrm{Re}\left(\sum_n a_n^{i\,*} Z_n - \frac{1}{2}\sum_n \sum_m a_n^{i\,*} a_m^i S_{n-m}\right)\right\}, \tag{3.31}$$

where,

$$Z_n = \int_I R(t)\,h^*(t - nT)\,dt\ , \tag{3.32}$$

$$S_{n-m} = \int_I h(t - nT)\,h^*(t - mT)\,dt \tag{3.33}$$

The result in Equation 3.31 is exactly the expression found in the classic paper by Ungerboeck [3] on maximum-likelihood reception. As stated before a single filter can now replace the bank of matched filters, shown in Equation 3.30 sampled at the symbol rate. The N samples in Equation 3.32 now become the sufficient statistics for detection of the transmitted sequence. Since it is assumed the CIR is known Equation 3.33 is just a set of known parameters that must be calculated. By whitening the expression in Equation

3.29 with a discrete whitening filter one can obtain a Euclidean distance metric exactly like the one found in the classic paper on maximum-likely receivers by Forney [8].

3.4 The Viterbi Algorithm

What is left, is the daunting task of calculating Equation 3.31 for each possible sequence. From the expression, one can see that the number of calculations grows exponentially with the length of the message. This would require extensive processing, and would be an obstacle in the implementation of the receiver. To be practical the number of calculations should be constant for each succeeding symbol. By using a modified version of the Viterbi Algorithm the calculations can be made proportional to $|\{a_n\}|^L$ where "*L*" is the truncated length of the CIR in symbol periods (T_s) and $|\{a_n\}|$ is the number of possible symbol values. To do this, first start by noting that the expression in Equation 3.31 can be manipulated to produce

$$\underset{\{a\}}{Max} \quad \{J_n(\{a_1, a_2, a_3, ..., a_N\})\}, \tag{3.34}$$

$$J_n = J_{n-1}(\{a_1, a_2, ..., a_{n-1}\}) + \mathrm{Re}[a_n^*(2Z_n - S_0 a_n - 2\sum_{l=1}^{L} S_l a_{n-l})] \ , \tag{3.35}$$

where the maximization in Equation 3.34 is taken over all possible sequences $\{a_i\}$. The expressions in Equation 3.34, and 3.35 show that the maximization can be accomplished recursively. First, the problem must be reformed.

Looking at the expression in Equation 3.35 one can see that for each sample this term can be seen as a representation of a FSM. The possible states are the symbols $a_{n-1}...a_{n-L}$ and the input to the FSM is the symbol a_n. For each possible state depending on

the input symbol the FSM will transition to a future or next state represented by the symbols $a_n \ldots a_{n-L+1}$, this continues until the last symbol in the message is received so the last state is then $a_N \ldots a_{N-L}$. The number of possible combinations of present state and future state assuming no coding is $|\{a_n\}|*|\{a_n\}|^L$. In the case of QAM with a CIR of length one (1), there would be 16 possible combinations. If one was to present this FSM graphically on a time scale it could be represented by a so-called trellis diagram. As can be seen in Figure 3.1, there are four possible states and from each state, there are four possible state transitions. The arrows emanating from each state and terminating at each of the four possible next states depict this. Going back to the expression in Equation 3.35 the value of the second term is the output of the FSM at each sample. Therefore each of the possible combinations of state $\{a_{n-1} \ldots a_{n-L}\}$ and input a_n, will be weighted. The weights associated for each of the possible paths through the trellis will be summed and the path with the largest summed weight will be chosen as the most likely sequence. The Viterbi Algorithm is perfectly suited for this type of problem, and is summarized below.

Consider a partial path metric given by $J_n\{a_o,a_1,\ldots a_n\}$ that terminates at one of the $|\{a_n\}|^L$ nodes of the trellis at time nT_s. All paths through this node must contain one of the partial paths that terminate there. Any path through this node has a metric, which can be written as,

$$\underset{0}{\overset{N}{J}}\{a_1, a_2, \ldots, a_N\} = \underset{0}{\overset{n}{J}}\{a_1, a_2, \ldots a_n\} + \underset{n+1}{\overset{N}{J}}\{a_{n+1}, a_{n+2}, \ldots, a_N\} \quad . (3.36)$$

The partial path terminating at this node with the largest partial metric (the first term on the RHS of Equation 3.36 must be part of the path which goes through this node and has the maximum path metric of all possible paths which go through this node, any

other path which goes through this node but has a smaller partial metric must have a smaller accumulated metric according to Equation (3.36). These paths are called survivor paths and are the only which need be retained for further calculation. Since it isn't know which of the possible states will be included in the path with the maximum metric a survivor path for each states must be retained.

The iterative process is now clear. Using Equation 3.35), start at "n=1" and retain only the survivor paths, then proceed with "n=2" and continue using Equation 3.36 until the end of the message has been reached. The path with the maximum metric at the last iteration is the most likely sequence.

This process is depicted in Figure 3.1, the survivor paths at each sample are the light dashed lines. Therefore, the solid arrows entering each state can be discarded when determining the most likely sequence. The heavy dashed line is the sequence estimated by the algorithm.

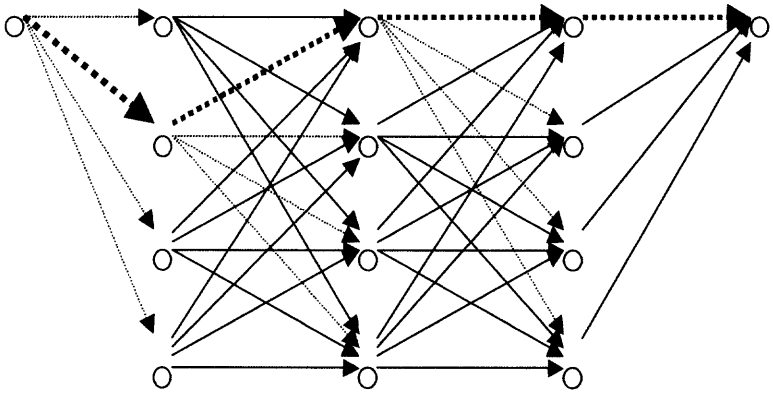

Figure 3.1 State Trellis for QPSK with channel memory of one symbol and message length of five.

What has been found in our derivation is the sequence that has the minimum probability of sequence error. That is the most likely sequence can contain any number of symbol errors, it may be one or one hundred.

As long as the accumulated metric is the maximum, it is considered most likely and will be used as the estimate without any consideration of the symbol errors. The symbol error rate, or at least a tight bound on it, can be determined through an exhaustive search for what is called a minimum error event. The details of this derivation will not be delved into in this thesis. Instead, simulations will be used to determine the maximum-likelihood receiver's performance. The interested reader can find the details in the references by Forney Ungerboeck and Proakis. All derivations are basically the same as the original by Forney. However, Proakis gives the most readable version of the three.

3.5 A Sub-Optimal MLSE Receiver

By inspection of Equation 3.30 one can see that the MLSE is comprised of two sections. The front end is comprised of a filter, matched to the CIR and sampled at the symbol rate. Following this is a sequence estimator implemented using the Viterbi algorithm. In the proceeding derivation, it was assumed that the CIR was known. In a real world implementation of the MLSE receiver, the CIR would have to be estimated. This adds complexity to the receiver especially if the CIR is changing at a rate comparable with the duration of the data block. One method used to simplify the implementation of the receiver is the use of a receive filter matched only to the transmit filter. This eliminates the need for tracking the overall CIR, which in general requires sampling at greater than

the symbol rate. This is sub-optimal of course since the CIR is a composite of the transmit filter response and the response of the channel but the reduction in complexity is significant.

There is also an added risk when implementing the receiver in this manner that in-band nulls can be formed due to ailising caused by symbol rate sampling of the receive filter. Nulls can form when the composite phase response comprised of transmit, channel and receive filters is asymmetrical. Ailising occurs using matched filter as well but the phase response at its' output is flat so there is no chance of the phases in the ailised portion of the response adding destructively. Never the less the reduction in performance can be compensated by a significant reduction in complexity. In the IS-136 standard the composite response of transmit and receive filters has a raised root cosine response so in the absence of a dispersive channel the response has zero ISI.

CHAPTER 4

COMBINED INTERFERENCE CANCELLER AND MLSE

4.1 Optimum Combined Interference Canceller and Channel Estimator Weights

4.1.1 Linear Constraints

In this section, the channel estimator coefficients and the antenna array weights are derived simultaneously using a direct matrix inversion (DMI) technique. This technique supplies an estimate of the results obtained using the statistical minimum mean square error criteria.

From Figure 1.4, we get,

$$\mathbf{Y} = X\mathbf{w} \ , \tag{4.1}$$

$$\mathbf{w} = [w_1, w_2, w_3, ...w_N]^T \ , \tag{4.2}$$

where **X** represents a matrix whose columns are the input signals to each of the 'N' antennas,

$$X = [\mathbf{x}_1, \mathbf{x}_2, \mathbf{x}_3, ...\mathbf{x}_N] , \tag{4.3}$$

$$\mathbf{x}_k = [x_k(0), x_k(1), x_k(2), ...x_k(L)]^T \ , \quad \text{L= length of the training sequence.} \tag{4.4}$$

Define the training sequence,

$$\mathbf{d} = [d(0), d(1), d(2), ...d(L)]^T , \tag{4.5}$$

$$d(n) = 0 , n<0.$$

To construct the modified training sequence, first define a matrix 'A' whose width is equal to the number of taps in the channel estimation (fir) filter. Each column of this matrix is a time delayed or time advanced version of the training sequence. Since the

overall channel response can have both a causal and non-causal component, the center tap of the estimation filter, **c,** will be used as the reference and the 'A' matrix will be defined as

$$A = [\mathbf{d}(n-u),...,\mathbf{d}(n),...\mathbf{d}(n+u)], \qquad \text{2u+1=Width of estimation filter.} \tag{4.6}$$

Given the definitions above the error function is,

$$\mathbf{e}^H\mathbf{e} = [X\mathbf{w} - A\mathbf{c}]^H[X\mathbf{w} - A\mathbf{c}]$$

$$\mathbf{w}^H X^H X\mathbf{w} - \mathbf{w}^H X^H A\mathbf{c} - \mathbf{c}^H A^H X\mathbf{w} + \mathbf{c}^H A^H A\mathbf{c} \tag{4.7}$$

$$\frac{\partial(\mathbf{e}^H\mathbf{e})}{\partial\mathbf{w}} = 2R_x\mathbf{w} - 2P\mathbf{c} = \mathbf{0} \tag{4.8}$$

$$\frac{\partial(\mathbf{e}^H\mathbf{e})}{\partial\mathbf{c}} = 2R_a\mathbf{c} - 2\mathrm{P}^H\mathbf{w} = \mathbf{0} \tag{4.9}$$

$$R_a = A^H A,\ R_x = X^H X,\ \mathrm{P} = X^H A. \tag{4.9a,b,c}$$

Inserting Equation 4.8 into Equation 4.9 the final expression for the filter coefficients is,

$$(R_a - \mathrm{P}^H R_x\mathrm{P})\mathbf{c} = \mathbf{0}. \tag{4.10}$$

As the expression in Equation 4.10 shows the optimum weights can converge to the all zeros vector, a useless result. Constraints on the coefficients will be used to eliminate this problem. For simplicity, a linear constraint on the filter coefficients of the form, $\mathbf{b}^T\mathbf{c}$ = a is used. Using the method of Lagrange the appended cost function Equation 4.7 becomes,

$$\mathbf{e}^H\mathbf{e} = [X\mathbf{w} - A\mathbf{c}]^H[X\mathbf{w} - A\mathbf{c}] + \upsilon\left(\mathbf{b}^T\mathbf{c} - a\right). \tag{4.11}$$

The expression in Equation 4.9 now becomes,

$$\frac{\partial(\mathbf{e}^H\mathbf{e})}{\partial\mathbf{c}} = 2R_a\mathbf{c} - 2\mathrm{P}^H\mathbf{w} - \upsilon\mathbf{b} = \mathbf{0}, \tag{4.12}$$

$$\mathbf{b}^T\mathbf{c} = a\,. \tag{4.13}$$

Inserting Equation 4.8 into Equation 4.12 and solving for **c** you have,

$$\mathbf{c} = \frac{\upsilon}{2}(R_a - \mathrm{P}^H R_x^{-1}\mathrm{P})^{-1}\mathbf{b}\,. \tag{4.14}$$

Inserting Equation 4.14 into Equation 4.13 and solving for υ gives,

$$\upsilon = \frac{2a}{\mathbf{b}^T(R_a - \mathrm{P}^H R_x^{-1}\mathrm{P})^{-1}\mathbf{b}}\,. \tag{4.15}$$

Finally **c** can be obtained by inserting Equation 4.15 into Equation 4.14 which gives,

$$\mathbf{c} = \frac{a(R_a - \mathrm{P}^H R_x^{-1}\mathrm{P})^{-1}\mathbf{b}}{\mathbf{b}^T(R_a - \mathrm{P}^H R_x^{-1}\mathrm{P})^{-1}\mathbf{b}}\,. \tag{4.16}$$

Inserting Equation 4.16 into Equation 4.8 produces an expression for the array weight vector,

$$\mathbf{w} = \frac{R_x^{-1}\mathrm{P}a(R_a - \mathrm{P}^H R_x^{-1}\mathrm{P})^{-1}\mathbf{b}}{\mathbf{b}^T(R_a - \mathrm{P}^H R_x^{-1}\mathrm{P})^{-1}\mathbf{b}}\,. \tag{4.17}$$

Using the expression in Equation 4.16 and the identity in Equation 4.9c, Equation 4.17 can be rewritten to give,

$$\mathbf{w} = R_x^{-1}X^H A\mathbf{c}\,. \tag{4.18}$$

The output from the array can now be obtained by inserting Equation 4.18 into Equation 4.1 which gives,

$$Y = XR_x^{-1}X^H A\mathbf{c}\,. \tag{4.19}$$

Noting that the first three terms on the LHS of Equation 4.19 produce a projection matrix the array output can be rewritten as,

$$Y = \Omega_x A\mathbf{c}\,, \tag{4.20}$$

where Ω_x is a projection matrix and the term Ac is the training sequence filtered by the channel estimation filter **c**. From Equation 4.20 it can be seen that analogous to the result for optimum combining [2] the output of the adaptive array **Y,** is the projection of the modified training sequence Ac, onto the observation-space. This is an intuitively pleasing result. Assuming the channel can be represented by a T-spaced Fir filter, and the vector **c** converges to the exact channel coefficients, the output from the array represents the best estimate of the modified training sequence **Ac.** Therefore, any signals uncorrelated with this sequence should be suppressed by the array, within the confines of the arrays degrees of freedom for signal suppression. If the channel estimation filter is an impulse then Equation 4.20 reduces to the same expression as given by [2]. It's clear that a constraint vector other then **c** can be selected. Intensive simulation has shown that $\mathbf{b} = [0\ 1\ 0]^T$ gives good results, hence such a choice will be included in the following comparison.

4.1.2 Eigen-Decomposition

Choosing a constraint of **b=c** forces the energy in the filter coefficients to equal some constant. With this Equation 4.14 becomes,

$$(R_a - \mathrm{P}^H R_x^{-1} \mathrm{P})\mathbf{c} = \frac{\lambda \mathbf{c}}{2} . \tag{4.21}$$

This eigenvector eigenvalue problem defines **c** as the eigenvector to the corresponding eigenvalue λ. By expanding the bracketed term in Equation 4.21 one gets,

$$(A^H(\mathrm{I} - XR_x^{-1}X^H)A)\mathbf{c} = (A^H \Omega_{X\perp}^H \Omega_{X\perp} A)\mathbf{c} = (\beta^H \beta)c , \tag{4.22}$$

where $\Omega_{X\perp}^{H}\Omega_{X\perp} = \Omega_{X\perp}$ is defined as the orthogonal projection matrix of the columns of X. The matrix β then becomes the projection of the columns of the matrix A defined in Equation 4.5), onto a vector space orthogonal to the observation vectors that make up the columns of the X. The matrix defined by $\beta^{H}\beta$ is an (2u+1)x(2u+1) Hermitian matrix and so it can be decomposed into the form $U\Lambda U^{-1}$ where $\Lambda \triangleq diag(\lambda_1, \lambda_2, ...\lambda_N)$, a diagonal matrix of eigenvalues and U is a unitary matrix, $(U^{H} = U^{-1})$ whose columns are the eigenvectors of the matrix $\beta^{H}\beta$. The question remains which eigenvector to select for the channel estimator. Inserting Equation 4.18 into Equation 4.7 and selecting the vector "**c**" that minimizes the mean square error we get after simplification,

$$MSE = \frac{a}{\mathbf{b}^{T}(R_a - \mathrm{P}^{H}R_x^{-1}\mathrm{P})^{-1}\mathbf{b}}. \tag{4.23}$$

Inserting Equation 4.21 into Equation 4.23 gives the result for the mean square error,

$$MSE = a\lambda. \tag{4.24}$$

From Equation 4.24 it's obvious that the eigenvector associated with the smallest eigenvalue should be selected as the channel estimator.

4.2 Proof of an Optimal Solution

A simple argument was presented will be shown as proof that the adaptive weights calculated as shown in the previous section will cancel uncorrelated interference while allowing the channel perturbed desired signal to pass through the array modified only by multiplication of complex constants. A short generalized proof will be presented below. *See Chapter 5 for details on the derivation of the channel model.*

To simplify the proof the following assumptions will be used. The desired signal is assumed to have the same multi-path delay profile but a different response at each antenna. Without loss of generality, assume that each interfering multi-path ray can be treated as an independent, flat faded interferer, the array must cancel.

The channel impulse response of the desired signal at antenna element x can be represented by,

$$h_x^0(kT) = \sum_{j=1}^{J} \alpha_{x,j}\, p(kT - \tau_j),\ k = -M,,0,,M, \tag{4.16}$$

where 2M+1 is the length of the T-spaced composite channel response and $p(t)$ is the combined receive and transmit filter response. The α_j in Equation 4.16 are the J multi-path complex iid random variables whose magnitudes have a Rayleigh distribution and whose phases are uniformly distributed between -π and π, and τ_j is the random delay associated with the j^{th} multi-path component.

From the assumptions described above, any interfering ray from a *single interferer* incident on an array element x can be represented as,

$$I_j(t) = \alpha_{x,j}\, p(t + \tau_i). \tag{4.17}$$

The desired signal component at the output of the array,

$$D(k) = \sum_{x=1}^{X} d(k) * \left[h_x^0(k) w_x\right], \tag{4.18}$$

d(k) being the T-spaced training sequence. The "T" has been dropped for convenience. At the output of the array any interference can be represented using Equation 4.17 as,

$$I = \sum_{j=1}^{Ji} \sum_{x=1}^{X} \alpha_{x,j} p(k - \tau_j) w_x \,, \tag{4.19}$$

where *Ji* is the number of multi-path rays incident on each array element. Using the error function defined in Equation 4.7 the mean square error at time "k", is in the case of no noise component,

$$MSE = E\left(\left| \sum_{x=1}^{X} d(k) * \left[h_x^0(k) w_x - c(k) \right] + \sum_{j=1}^{Ji} \sum_{x=1}^{X} \alpha_{x,j} p(k - \tau_i) w_x \right|^2 \right). \tag{4.20}$$

Which is zero when,

$$c(k) = \sum_{x=1}^{X} h_x^0(k) w_x \text{ , and } \sum_{j=1}^{Ji} \sum_{x=1}^{X} \alpha_{x,j} p(k + \tau_j) w_x = 0$$

$$\text{for } Ji < \mathrm{X} \,. \tag{4.21a,b}$$

Therefore, the error will be minimized when the adaptive Fir filter response *"c(k)"* is equal to the combined channel response modified only by multiplication of the complex weights w_n, which are chosen such that they cancel the interfering rays incident on the array. In this way the array passes the channel perturbed desired signal and cancels dispersive interferers provided the number of interfering multi-path rays are less than the number of antenna array elements. This ends the abbreviated proof.

4.3 Simulation Results

Below are the results from simulations run for channels where the desired user was subject to delay spread, but the interferers suffered only from frequency-flat fading. As stated previously, unless indicated, all simulations assume the channel is static over the interval of interest. Details about the channel model used for the simulations along with the theoretical considerations are presented in Chapter 5. The first figure shows the performance of cancellers for a channel with no delay spread. In the simulation, the canceller acts as a front-end processor, which feeds a simple differential detector. For Figure 4.1 and Figure 4.2 + = a single antenna, o = Canceller/Differential Detector with b = $[0\ 1\ 0]^T$, * = Canceller/Differential Detector with b = c, x = single tap Optimum Combiner/Differential Detector. For Figure 4.3 and Figure 4.4 x = 5-Tap OC/Differential Detector.

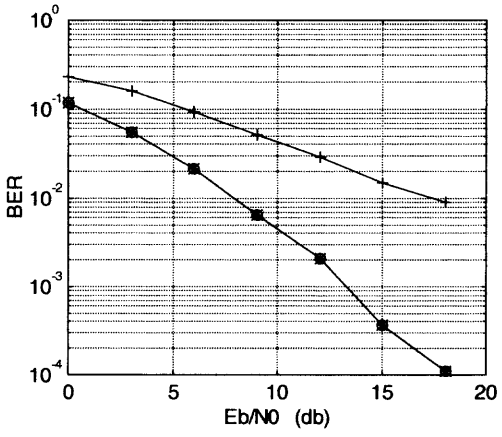

Figure 4.1 Performance of arrays in flat fading with differential detection.

The reason for this simulation is to prove that for this degenerative case the canceller reduces to a structure whose performance is equal to OC. The results are shown above in Figure 4.1. The simulation in Figure 4.2 is for the same channel except for the

addition of one equal power interferer. As in the case of the previous graph, all of the structures perform equivalently.

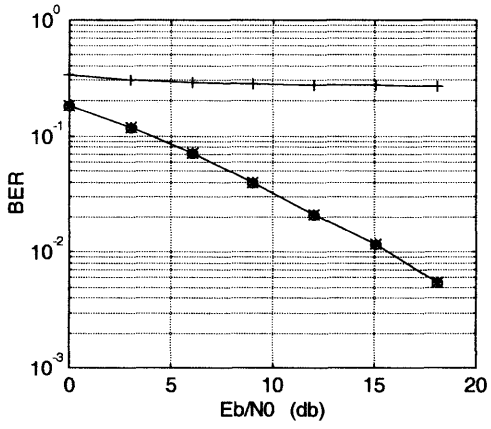

Figure 4.2 Performance of arrays in flat fading with differential detection and one equal power interferer.

To investigate the performance of our proposed receiver, the Canceller/MLSE, additional simulations were performed for a variety of channel impairments. The first simulation is shown in Figure 4.3, the results are for a two-ray channel with inter-ray

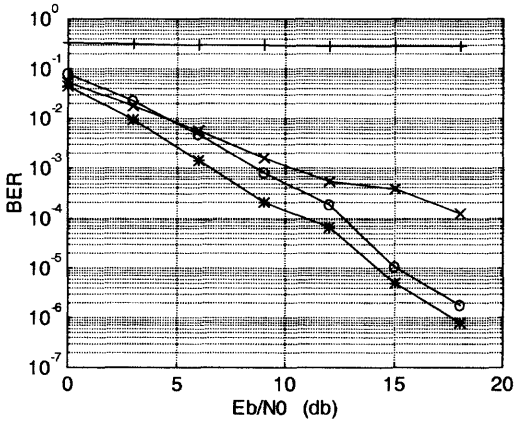

Figure 4.3 Performance of receivers for a two-path Ts-spaced channel with no interferer.

delay of one symbol period, interference is from one frequency-flat faded co-channel interferer.

The results in Figure 4.3 and Figure 4.4 show that the Canceller/MLSE performs much better than the 5-Tap OC regardless of whether or not an interferer is present. The data also shows that the eigen-decomposition technique outperforms the Canceller/MLSE with a linear constraint on the estimator coefficients. Additional simulations have found that when one imposes constraints on the array weights, or a combination of constraints on the array and estimator coefficients, the performance of the Canceller/MLSE is degraded. For this reason all Canceller/MLSE designs presented in this thesis use constraints on the estimator coefficients alone. Additional simulations are presented at the end of Chapter 5.

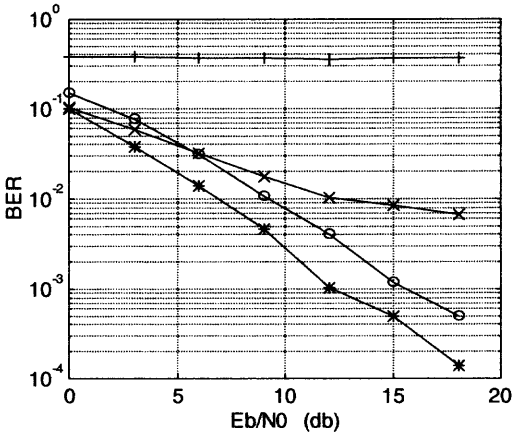

Figure 4.4 Performance of receivers for a two-path Ts-spaced channel with one flat faded interferer.

It's reasonable to assume a model of the mobile radio environment in which the interference signals are also subject to multi-path propagation. The space-time processor must be able to deal with these additional interfering signals.

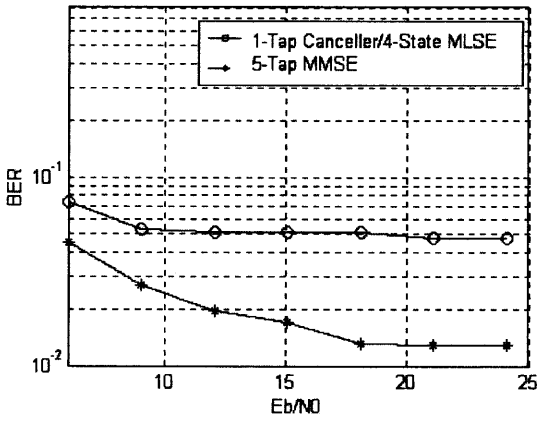

Figure 4.5 Multi-path propagation of an interfering signal.

For a simple two-element array, an interferer with additional multi-path ray components cannot be completely suppressed, so performance is degraded. This is shown graphically in Figure 4.5. The desired signal was subject to a two-path channel with inter-ray delay of T_S. Interference was from a single dispersive interferer with two multi-path components. The graph on the left shows results for an interferer with no delay spread, and is included for reference only. The drop in performance shown in the graph on the right of Figure 4.5 can be attributed to the limited available degrees of freedom the space-time processors have for interference cancellation and equalization. While both the five-tap MMSE (OC) and the Canceller/MLSE suffer from a loss in performance, the loss suffered by the Canceller/MLSE is much greater. The reason for this is simple; the Canceller/MLSE has fewer array coefficients to utilize to combat the dispersive interferer. Therefore the signal the canceller feeds the MLSE will have a higher contribution from interference than will the signal at the output of the MMSE (OC). Without some modification to the existing structure, the Canceller/MLSE would not be practical for many real applications.

4.4 Enhancements for Interferers with Delay Spread

The need to enhance the Canceller/MLSE is evident from the argument presented in the previous section. The question now is, what if any, enhancements to the original design can be made to accommodate dispersive interferers. Two methods to improve the Canceller's performance when dealing with dispersive interference have been proposed. The first is the simple addition of an antenna element in the array. While this only improves the array's spatial processing capability, it has been assumed the multi-path components are correlated between antenna elements. Therefore, the canceller should be able to treat each interfering multi-path component as an additional interferer that the array needs to suppress, improving overall performance. The second method uses the addition of temporal taps in the canceller array. It has been found though that a constraint on the channel estimator is necessary when additional temporal taps are added. The reason for this will be explained in the following sections along with supporting data from simulation. Additional simulation data is presented at the end of Chapter 5.

4.4.1 Additional Array Antennas

The addition of antenna elements to the array is the simple modification to improve performance, given that each of the interferering multi-paths can be considered iid in time, and spatially correlated. The practical considerations can be much more complicated, the availability of space for more than two antennas on a mobile unit is one issue which must be addressed. There is a variety of other implementation issues, which may make the addition of antennas to the mobile unit impractical. With the

aforementioned in mind, simulations have been conducted in which only one additional antenna has been included in the antenna array.

The simulations presented in this section are for canceller arrays with three antenna elements, one additional element more than the structures already presented in previous sections. In all the simulations, the signals at each antenna have been assumed to be spatially uncorrelated when averaged over a time interval much longer than a symbol period. Results of a few simulations are shown below in Figure 4.6.

As expected a single two-path interferer is completely cancelled, this is due to the additional degree of freedom for interference cancellation the array has gained with the inclusion of one more antenna.

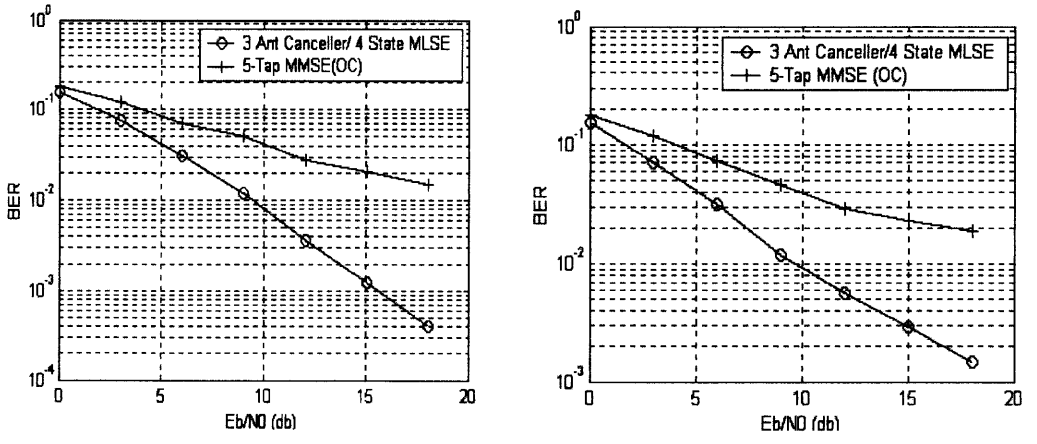

Figure 4.6 Performance for a Ts-spaced channel with a two-path (left), or three-path equal power interferer.

A more interesting result is the performance the three-antenna canceller has when subject to a single interferer with more than two multi-path components. Even though the canceller cannot eliminate the interferer, it does sufficiently suppress the interferer's multi-path to a point where adequate performance, which in the case of an IS136 system

is usually taken in the literature as a BER of 10^{-2}, can be obtained. This is shown in Figure 4.7 where the desired-users and interferer's SNR has been set to 17 db, and number of interfering multi-path rays has been increased to investigate the effect this has on performance.

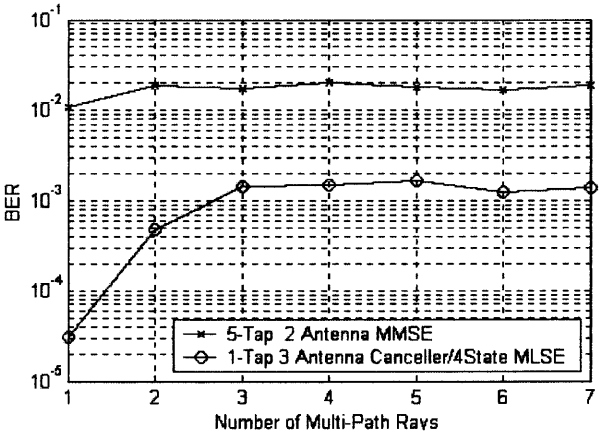

Figure 4.7 Performance of receivers for channel with one interferer.

4.4.2 Addition of Temporal Array Taps

A more practical method to combat dispersive interference is the addition of temporal taps to the canceller array, since this can be done with software alone. Implementing a canceller with temporal taps is simply a matter of modifying the equations given in section 4.1.1 to accommodate temporal coefficients. A center-tap reference for the array filters has been chosen, so the governing equations take on the forms shown below. Referring to Equations 4.1 to 4.4 and Figure 1.4, we have,

$$\mathbf{Y} = X\mathbf{w}\,. \tag{4.21c}$$

Expanding the coefficient vector to include temporal taps, we get,

$$\mathbf{w} = [w_1, w_2, w_3, \ldots wm_N]^T, \tag{4.22}$$

and,

$$X = [\mathbf{x}_1, \mathbf{x}_2, \mathbf{x}_3, \ldots \mathbf{x}m_N]. \tag{4.23}$$

In Equations 4.22 and Equation 4.23 "N" refers to the number of antenna elements, while "M" is the number of temporal taps at each antenna. Therefore, the total number of canceller coefficients has now become "N*M".

Given that the filters at each antenna have a center-tap reference, and that each filter has (M+1)/2 causal and non-causal taps, the vectors in Equation 4.23 can be grouped into "M" columns such that they take on the following form for the k[th] antenna,

$$\Theta_K = [\mathbf{x}^k_{n-(m-1)/2,}, \ldots, \mathbf{x}^k_{n-1,} \mathbf{x}^k_{n,} \mathbf{x}^k_{n+1,}, \ldots, \mathbf{x}^k_{n+(m-1)/2,}], \qquad k = 1,2,3,\ldots,N, \tag{4.24}$$

so that Equation 4.23 can be rewritten as,

$$X = [\Theta_{1,} \Theta_{2,} \Theta_{3,} \Theta_{4,} \ldots\ldots \Theta_{N,}]. \tag{4.25}$$

The vectors in Equation 4.24 are written as,

$$\mathbf{x}^k_{n-v} = [x^k(n-v), x^k(n-v-1), x^k(n-v-2), \ldots, x^k(n-v-L)]^T \ , \ v = \text{-}(m\text{-}1)/2 \text{ to } (m\text{-}1)/2. \tag{4.26}$$

To investigate the performance of the canceller with the addition of temporal taps simulations have been performed for a variety of environmental scenarios. Some of the results are shown below in Figure 4.8 and Figure 4.9. One can plainly see that the performance of this structure is poor when a simple four state trellis is used in the MLSE. It is necessary to increase the complexity of the MLSE by increasing the state trellis from four to sixteen states in order to obtain reasonable performance. Although, for modern

digital signal processing equipment a sixteen state trellis is not too complex to be implemented, the graph in Figure 4.9 shows a flaw in this design. In the graph the user is subject to flat fading only, yet the canceller/mlse without temporal taps significantly outperforms the canceller with temporal taps. One would expect, in this case, that

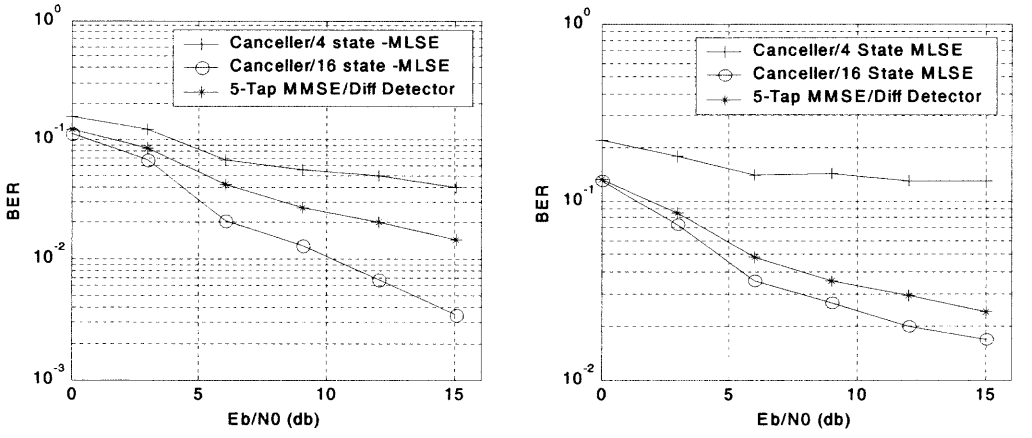

Figure 4.8 Performance of receivers for a symbol spaced channel with one equal power interferer subject to a two-path Ts spaced channel (left), and three-path Ts/2 spaced channel.

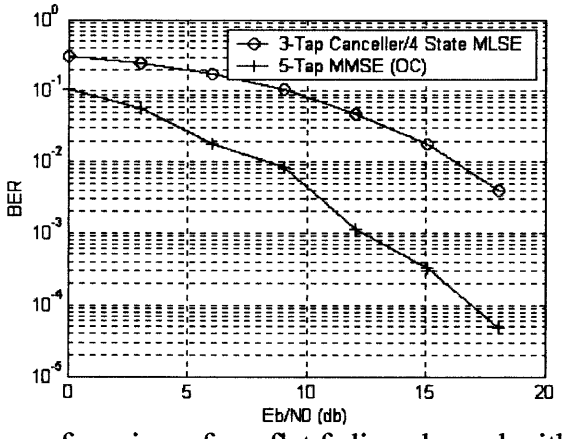

Figure 4.9 Performance of receivers for a flat fading channel with no interference.

the two structures would have similar performance. To find the reason why these structures perform differently one needs to look at Equation 4.20, and modify it for a canceller with temporal taps. The revised expression is given by,

$$MSE = E\left(\left|\sum_{x=1}^{X} d(k) * \left[h_x^0(k) * w_x(k) - c(k)\right] + \sum_{j=1}^{Ji}\sum_{x=1}^{X} \alpha_{x,j} p(k-\tau_j) * w_x(n)\right|^2\right) \tag{4.27}$$

In the absence of interference the expression is given by,

$$MSE = E\left(\left|\sum_{x=1}^{X} d(k) * \left[h_x^0(k) * w_x(k) - c(k)\right]\right|^2\right). \tag{4.28}$$

Which is minimum when,

$$\sum_{x=1}^{X} h_x^0(k) * w_x(k) = c(k). \tag{4.29}$$

From Equation 4.29, to minimize the MSE the channel estimator and the sum of the convolution of the array filters and the channel responses need to be equivalent. There is no constraint on any of the coefficients, so either the channel estimator or the array filters, or both may have both causal and non-causal components. This can result in a sort of spreading of the channel estimator, which would make it necessary to increase the number of states in the MLSE to compensate for the longer channel response. Investigating the flat faded case shown in Figure 4.9, it was found that the channel estimator had both causal and non-causal components, which would require a higher state trellis. This is the cause of the performance degradation.

To compensate for the problem of estimator spreading a constraint on the channel estimator has been proposed. The estimator has been constrianed to be causal, with a memory of one. In other words, a two tap estimator with just one causal tap. This is reasonable for a four state MLSE trellis. The estimator and array coefficients are optimizated, as was done previously, using the eigen-decomposition technique to find the estimator coefficients and Equation 4.18 to find the array weights. Simulations have been conducted for the same environmental scenarios as before, but this time with the aforementioned constraint on the channel estimator, the results are shown below.

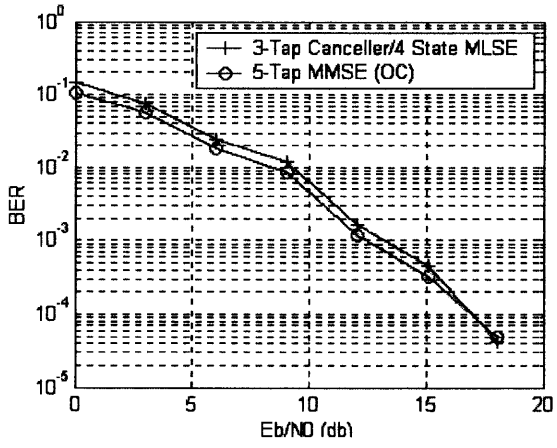

Figure 4.10 Performance of receivers for a flat fading channel with no interference.

From the results in Figure 4.10 and Figure 4.11, one can see that there is a significant improvement in the performance of the Canceller/MLSE when a constraint is imposed on the channel estimator. The question to ask next is whether the addition of temporal taps can be used obtain performance equivalent to the three-antenna canceller. This would require an increase in the complexity of the canceller, but the performance improvement would be without the need for any additional hardware. This is what is the

focus of the simulation in Figure 4.13. The worse case scenario has been used from Figure 4.12, which is a two-path Ts-spaced channel and a single interferer with seven multi-path rays. For this simulation, an odd number of array-taps uses a center tap reference while an even number has one more non-causal tap. The graph shows that a canceller with five temporal taps outperforms the three-antenna configuration, and that the addition of more than five taps does little to improve performance.

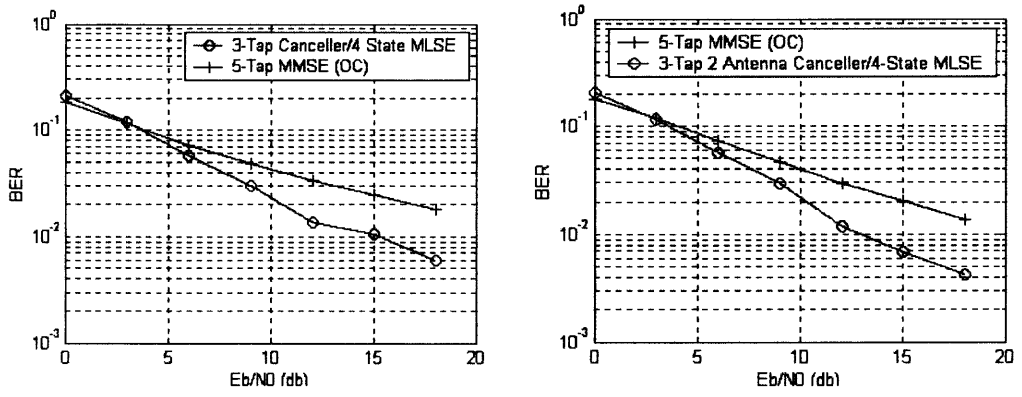

Figure 4.11 Performance for a two-path Ts-spaced channel with one equal power interferer with a two-path Ts-spaced channel (right), and a three-path Ts/2-spaced channel.

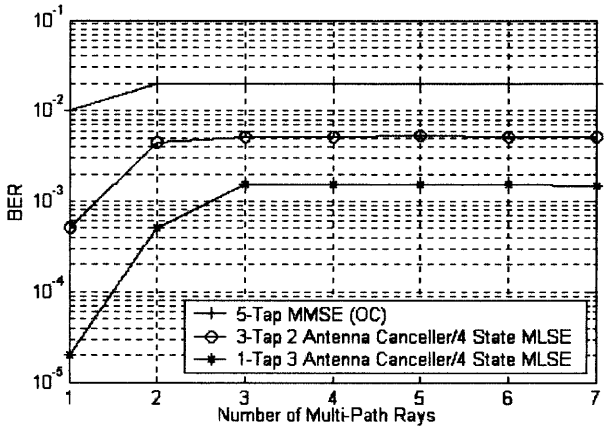

Figure 4.12 The addition of multi-path components to one equal power interferer for a two path, T_s-spaced channel with Eb/N_0= 17 db.

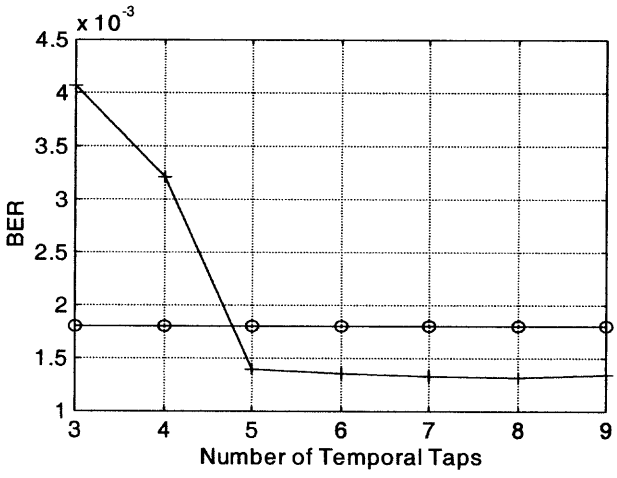

Figure 4.13 Performance of receivers for Eb/N0 = 17 db, and one 7-path equal power interferer.

CHAPTER 5

SIMULATIONS

5.1 The Mobile Radio Channel

In a typical mobile radio environment, the signal transmitted from the base station will follow many different paths to reach the mobile receiver. The number of paths is usually very large and each will impose a variation on the signal. In general, each signal arrives at the mobile receiver at a different time and may undergo a change in phase and amplitude before arriving at the mobile. This is depicted graphically in Figure 5.1, where a limited number of paths have been shown for simplicity. The buildings obstructing the direct path show how this scattering of the signal may occur.

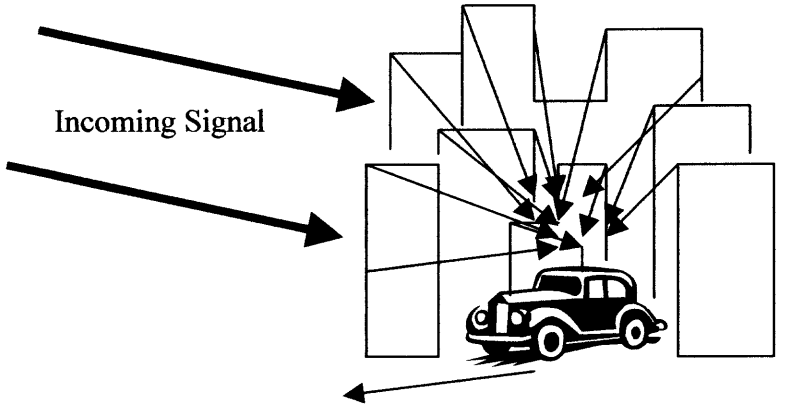

Figure 5.1 Scattering of the incoming signal.

The signal received at a mobile can be modeled as the superposition of many waves arriving from different directions and with different relative delays. The delays are measured relative to the first wave incident on the receiving antenna. A signal transmitted

at frequency w_0 would arrive as a superposition of N*M*L waves, each from one of N angles in the horizontal plane, M angles in the vertical plane and with L delays. The electric field at the receiver can be written as,

$$E(t) = E_0 \sum_{l=1}^{L} \sum_{m=1}^{M} \sum_{n=1}^{N} C_{nml} \cos(w_0 t + w_{nm} t - w_0 T_{nml}) \ , \tag{5.1}$$

where,

$$w_{nm} = 2\pi f_d \cos(\gamma - \Phi_n) \sin(\theta_m) \ , \tag{5.2}$$

and,

$$C^2_{nml} = G(\theta_m, \Phi_n) p(\theta_m, \Phi_n, T_{nml}) d\theta d\Phi dT \ . \tag{5.3}$$

The term f_d is the maximum Doppler frequency given by the relationship $f_d = v/\lambda$, where v is the velocity of the mobile and λ is the wavelength of the carrier frequency f_0.

The "f_d"term in Equation 5.2 is referred to as the Doppler frequency. Figure 5.2 depicts graphically how this term comes about.

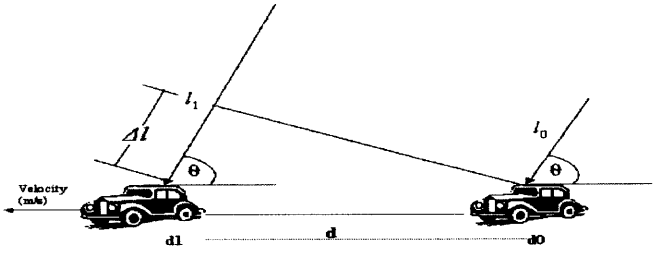

Figure 5.2 The Doppler effect.

In the figure, the box labeled with d_0 is the position of the mobile at some reference time. The mobile travels with velocity v and in an elapsed time Δt has traveled

a distance "d" to position d_1. If the transmitter is assumed to be far from the mobile, the signal will impinge on the mobile's antenna at approximately the same angle θ at both positions. The distance traveled by the signal from the base station to the mobile at position d_0 is shown in the figure as l_0, and l_1 at the position labeled d_1. For simplicity, assume the signal is an un-modulated carrier at frequency w_0. The phase of the signal at time t_0 is calculated as $w_0(t_0 + \frac{l_0}{c})$ and, $w_0(t_1 + \frac{l_0 + \Delta l}{c})$ at time t_1. The term c is the speed of light, $3x10^6$ (m/s). The frequency of the carrier over the time interval Δt is the change in phase over Δt,

$$\frac{\Delta\theta}{\Delta t} = \frac{w_0}{\Delta t}(\Delta t - \frac{\Delta l}{c}), \tag{5.4}$$

$$= w_0 + \frac{2\pi}{\Delta t}(\frac{\Delta l}{\lambda}). \tag{5.5}$$

From the figure Δl can be written as $d\cos(\theta)$, or $v\Delta t\cos(\theta)$, where v is the velocity of the vehicle. Substituting for Δl Equation 5.5 now becomes,

$$w = w_0 + \frac{2\pi v\cos(\theta)}{\lambda}. \tag{5.6}$$

The second term in Equation 5.6 is called the Doppler frequency and is dependent on the vehicle's speed, the wavelength of the carrier frequency and the angle at which the signal arrives at the mobile with respect to the direction of the mobile's motion. Each of the constituent waves that comprise the signal will have a Doppler frequency. The actual frequency is a random variable that is governed by the angular distribution of the arriving waves as shown in Equation 5.2. For analysis, assume that there is no deterministic component in the arriving signal. The effect of a deterministic component would be to

modify the statistical distribution of the signal's envelope, which will be discussed shortly. From Equation 5.6 the Doppler frequencies can vary between, 0 and $\frac{2\pi v}{\lambda}$ Radians. In real world situations, the maximum Doppler frequency plays an important role. It has been shown [33] that the maximum Doppler frequency approximates the frequency at which the signal strength of the signal will fade from its mean value.

The first term on the RHS of Equation 5.3 is the gain pattern for the receiving antenna. In our analysis, this function will be assumed unity for all angles. This of coarse is not possible in practice but is used often in analysis since it greatly simplifies calculations, so it is used here as well. Equation 5.1 can be re-written as,

$$E(t) = E_0 \sum_{l=1}^{L} \sum_{m=1}^{M} \sum_{n=1}^{N} C_{nml} \cos(w_{nml} t - w_0 T_{nml}) \cos(w_0 t) - E_0 \sum_{l=1}^{L} \sum_{m=1}^{M} \sum_{n=1}^{N} C_{nml} \sin(w_{nml} t - w_0 T_{nml}) \sin(w_0 t) . \tag{5.7}$$

By the central limit theorem, the two triple sums in Equation 5.7 are Gaussian distributed random processes, and are jointly Gaussian. With this in mind the received electric field at the mobile can be written as,

$$E(t) = x_I(t) \cos(w_0 t) - x_Q(t) \sin(w_0 t), \tag{5.8}$$

where $x_I(t)$ and $x_Q(t)$ are the jointly Gaussian random processes described by the distribution,

$$\mathrm{P(x)} = \frac{1}{\sqrt{2\pi}} e^{-\frac{x^2}{2}}, \qquad -\infty < \mathrm{x} < \infty . \tag{5.9}$$

. An equivalent representation for the signal in Equation 5.8 can be written as,

$$E(t) = \mathrm{Re}\{r(t) e^{iw_0 t}\}. \tag{5.10}$$

where, $$r(t) = x_I(t) + ix_Q(t), \tag{5.11}$$

is the equivalent base-band representation of the pass-band signal $E(t)$. It has been shown that the magnitude of random variable *r(t) (i.e.:| r(t)|)* follows a Rayleigh distribution given by [25],

$$P(r) = \frac{r}{\sqrt{2\pi}} e^{-\frac{r^2}{2}}, \qquad r > 0, \tag{5.12}$$

while the phase, $\angle r(t)$ follows a uniform PDF [25].

$$P(\Phi) = \frac{1}{2\pi}, \qquad 0 < \Phi \leq 2\pi. \tag{5.13}$$

5.1.2 Narrowband Channel Characteristics

For the work presented in this thesis the receiver has been assumed to be narrowband. By narrowband, it means that the receiver's limited bandwidth cannot distinguish between individual multi-path waves whose differential delay is small compared to the inverse of the receiver's bandwidth Given this condition the receiver will interpret these delayed signals as one composite wave which can be described by Equation 5.7). With the modification that the delay terms be replaced by constants.

An example is shown in Figure 5.3. The first pulse, shown as the dashed line is the summation of twenty-five equal-energy square-root-raised-cosine pulses centered at approximately one eighth of a second. Each wave is separated by one eightieth of the inverse of the pulse bandwidth. The second pulse, shown as a solid line, is a single square-root-raised-cosine pulse centered at approximately one eighth of a second. The

two waves have been normalized so they have equal energy. For all practical purposes, the waves are identical.

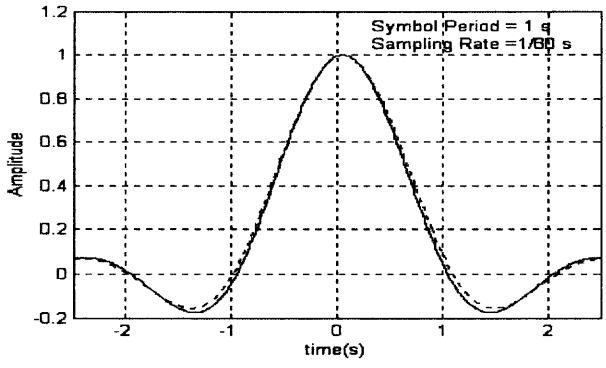

Figure 5.3 Creation of a composite wave due to the narrow-bandwidth of the mobile receiver.

In Figure 5.4, this concept has been extended by plotting three signals. The first signal, shown a with dashed line, is a summation of one hundred and twenty equal-energy square-root-raised-cosine pulses centered at approximately three quarters of a second. The second, shown with a dotted line, is the summation of two equal-energy square-root-raised-cosine pulses centered at three eights and nine eights respectively. The center of this two-pulse composite wave is three quarters of a second, which is the center of the first pulse as well. The last curve shown in the figure is a single square-root-raised-cosine pulse centered at three quarters of a second.

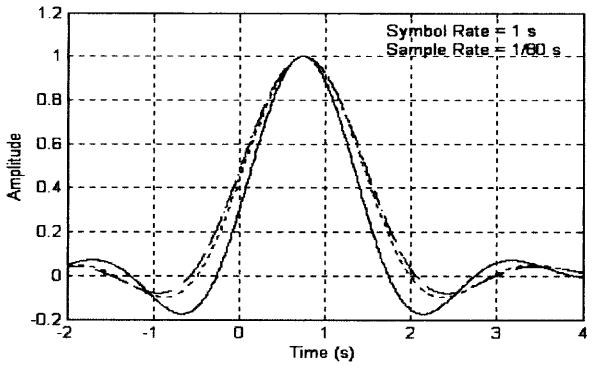

Figure 5.4 Creation of a multiple composite waves due to the narrow-bandwidth of the mobile receiver.

The figure above plainly shows the first composite wave can be approximated by two equal-energy waves separated by two thirds of the symbol period. The single pulse is no longer an accurate representation for the composite wave shown as the first curve. With the information from Figure 5.3 and Figure 5.4, one can see that when there are many waves spread over a small period of time compared to the inverse of the receiver's bandwidth, which in the case shown above is approximately T_s^{-1}, a single pulse representation is adequate, Figure 5.3. When the arriving waves are sufficiently spread out in time, as in Figure 5.4, the single pulse representation is no longer accurate and a multi-pulse composite wave must be used. Therefore for the purpose of simulation the signal received at the mobile antenna can be modeled as a composite wave comprised of two or more signals each with a form described by Equation 5.7 with the modification that the delay terms be replaced by a constants and the statistical nature of them dismissed in analysis. This is depicted graphically below in Figure 5.5. In an actual mobile environment, the signals arrive at the mobile antenna in a much more complicated

manner. The model has been greatly simplified, and has been included for discussion purposes only.

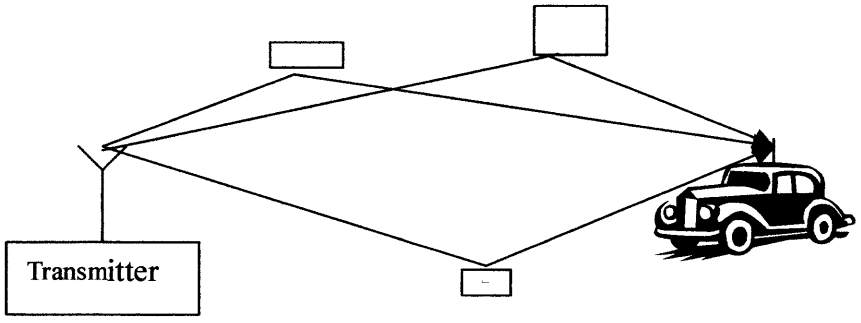

Figure 5.5 Multi-path propagation scenario.

The signal received by the mobile can now be defined as the sum of distinguishable composite multi-path rays each of the form given by Equation 5.11). Therefore, the channel impulse response for a particular receiving antenna element x will have the form,

$$g(t) = \sum_{j=0}^{J} \alpha_{x,j} \delta(t - \tau_j). \tag{5.14}$$

where the α_j's are the Rayleigh coefficients whose magnitude and phase distributions are given by Equation 5.12 and Equation 5.13 respectively, and the τ_j's are delays relative to the first arriving wave, τ_0, at the receiver. In this thesis, the delay between the arriving rays was varied to examine the influence the variation has on the performance of the receivers studied, but the delay was limited to no greater then one-symbol period. This is

a reasonable assumption given the simulations are for TDMA systems designed using the IS-136 standard, which uses a symbol period of 41.1us.

5.1.3 Correlation Properties of Base-band Components

From the previous section a Rayleigh distribution for the envelope of the base-band channel and a uniform distribution for the phase has been accepted as the appropriate model for the simulations presented in this thesis This model assumes that there is no direct path from the transmitter to the receiver for any of the multi-path rays. If a direct path were considered the model would have an envelope that followed a Ricean Distribution. There are many more channel models, the interested reader can find useful information in the references given in [30,32]

The correlation properties of the base-band components will now be examined. These findings will show that antennas separated a distance of at least half a wavelength are approximately uncorrelated. In subsequent chapters, it will be shown how these uncorrelated signals can be used to combat signal fading and supply what is referred to as diversity gain.

In [31] the author shows that the correlation function for the signal in Equation 5.7 can be expressed as,

$$\int_0^{\pi}\int_0^{2\pi} P_0\, p(\Phi,\theta)\cos(2\pi f d_{\max}\cos(\gamma-\Phi)\tau)\sin(\theta)\,d\theta\,d\Phi \quad , \qquad (5.15)$$

where $p(\Phi,\theta)$ is the joint distribution of the azimuth and elevation angles.

The cross correlation between the in-phase and quadrature components of the complex envelope can be written as,

$$\int_0^{\pi}\int_0^{2\pi} P_0\, p(\Phi,\theta)\sin(2\pi f d_{\max}\cos(\gamma-\Phi)\tau)\sin(\theta)\,d\theta\,d\Phi\,. \qquad (5.16)$$

If the azimuth and elevation angles are considered statistically independent of one another, and that the elevation angle is distributed as $\delta(\theta-\pi/2)$ (i.e.: waves arrive in horizontal plane only) than the results in Equation 5.15 and Equation 5.16 reduce to,

$$a(\tau) = \int_0^{2\pi} P_o p(\Phi)\cos(2\pi f d_{\max}\cos(\gamma-\Phi)\tau)\,d\Phi\,, \qquad (5.17)$$

$$c(\tau) = \int_0^{2\pi} P_o p(\Phi)\sin(2\pi f d_{\max}\cos(\gamma-\Phi)\tau)\,d\Phi\,. \qquad (5.18)$$

Now the complex correlation function can be defined as,

$$\Gamma rr\,(\tau) = a\,(\tau) + ic\,(\tau)\,. \qquad (5.19)$$

as in [31]. Note that both the autocorrelation, and the cross-correlation functions defined above are defined by the distribution of the azimuth angle of arrival. If now a uniform distribution for the angle of arrival, $p(\Phi)$ in Equation 5.17 and Equation 5.18 is considered the resultant complex correlation function is Clarke's 2-d isotropic scattering model given by [32],

$$\Gamma rr(\tau) = 1/2\pi \int_0^{2\pi} P_o\cos(2\pi f d_{\max}\cos(\gamma-\Phi)\tau)\,d\Phi \qquad (5.20)$$

Equation 5.20 is a zero-order Bessel function of the first kind and is represented in the literature as,

$$J_0(x) = 1/2\pi \int_0^{2\pi}\cos(x\cos(\Phi))\,d\Phi\,. \qquad (5.21)$$

Therefore using Equation 5.21 the complex correlation function reduces to a real expression given by ,

$$\Gamma rr(\tau) = P_0 J_0(2\pi f_{d\max}\tau). \tag{5.22}$$

By substituting $f_{d\max}\tau$ with $v\tau/\lambda$ the expression in Equation 5.22 can be re-written as,

$$\Gamma rr(\tau) = P_0 J_0(2\pi v\tau/\lambda). \tag{5.23}$$

A graph of Equation 5.22 is shown below in Figure 5.6 for a normalized delay such that $v\tau$,the distance travel by the mobile is replaced by a single variable lambda, and the amplitude of the correlation function is normalized to one. Figure 5.6 clearly shows that for antenna separations greater than ½ a wavelength the between base-band components are approximately uncorrelated.

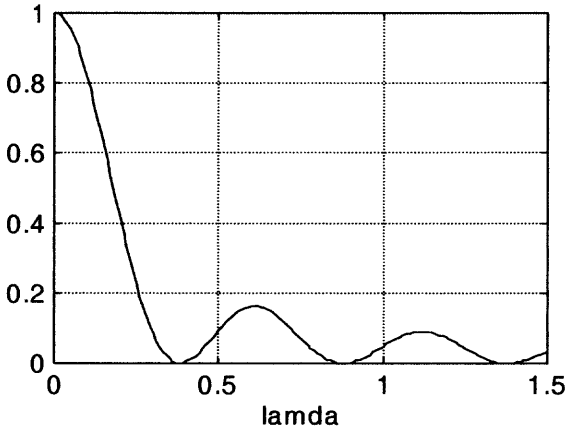

Figure 5.6 Theoretical covariance function of the complex envelope.

5.1.4 Spectrum of Base-band Components

Since the received signal was assumed wide-sense-stationary, the frequency spectrum of the base-band signal can be determined by simply taking the Fourier transform of Equation 5.23 with respect to τ, instead the derivation by Jakes [24] will be used, which

yields the same result. The derivation begins by noting the relationship between the received frequency and incident angle shown in Equation 5.6). This relationship can be written as,

$$f(\phi) = f_{d\max}\cos(\phi). \tag{5.24}$$

Where f_{dmax} is the maximum Doppler shift given by $\frac{2\pi v}{\lambda}$. From Equation 5.3), the fraction of the power incident on an antenna in the incremental angle $\partial\phi$ can be denoted $p(\phi)\partial\phi$. The differential power variation with frequency may be expressed as $S(f)\partial f$. Using Equation 5.24), which shows the relationship between frequency and angle of incidence, the following relationship can be made for a dipole antenna,

$$S(f)\partial f = 1.5[p(\phi) + p(-\phi)]\partial\phi, \tag{5.25}$$

$$S(f) f_{d\max}\sin(\phi)\partial\phi = 1.5[p(\phi) + p(-\phi)]\partial\phi. \tag{5.26}$$

But from Equation 5.24 $\sin(\phi)$ can be written as $\frac{\sqrt{f_{d\max}{}^2 - f^2}}{f_{d\max}}$ so Equation 5.26 becomes,

$$S(f) = \frac{1.5[p(\phi) + p(-\phi)]}{\sqrt{f_{d\max}{}^2 - f^2}}. \tag{5.27}$$

The assumption of a uniform distribution of power as a function of the angle of incidence when inserted into Equation 5.27 gives the final expression for the spectrum of the base-band components as,

$$S(f) = \frac{1.5/\pi}{\sqrt{f_{d\max}{}^2 - f^2}} \quad , |f_{dmax}| < f. \tag{5.28}$$

This expression is displayed in Figure 5.7 for an f_{dmax} equal to 100 Hz. The singularity at f_{dmax} in the response has been smoothed to enable a realizable implementation.

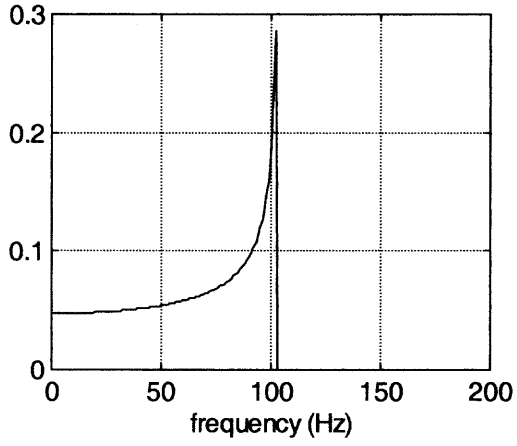

Figure 5.7 Jakes' one-sided Doppler spectrum of the base-band components. For a f_{dmax} of 100 Hz.

5.2 System Model

Given the theoretical analysis presented in previous sections of this chapter, the mobile channel model used in this work can now be defined. Focusing on the IS136 TDMA digital communications standard, which is a narrowband system, the expression in Equation 5.14 will be adequate for simulations presented in this work. The simulations are done at base-band, assuming timing and phase variations to be non-existent. This greatly simplifies the model. Another simplification was to assume the same delay profile at each antenna element in the array, a reasonable assumption, and one that is

commonly used in the literature. The final assumption is one of statistical independence between antenna elements, which can be attained in a real system given certain physical relationships between antenna elements are maintained. With the aforementioned in mind, a graphical representation of the model is presented in the Figure 5.8 shown below.

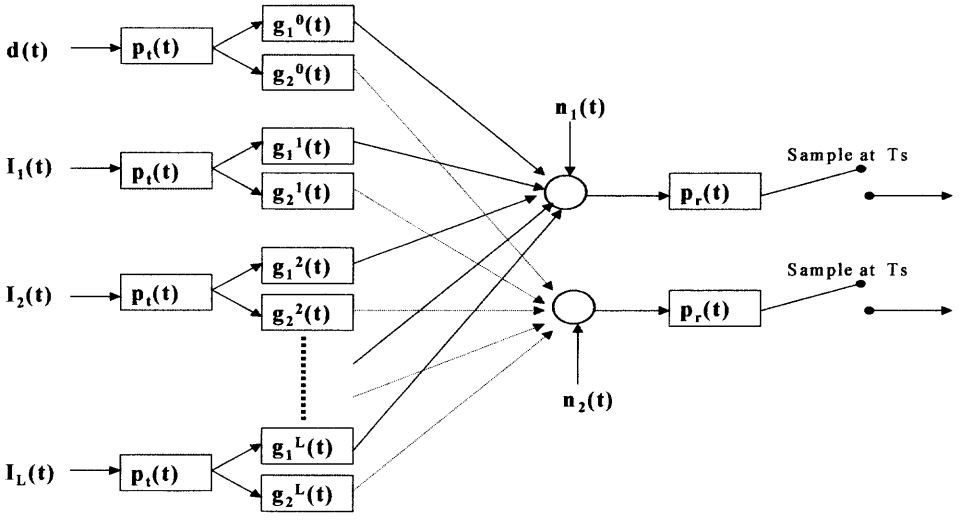

Figure 5.8 Two-antenna, base-band system model.

Using the model in Figure 5.5, the signal observed at antenna x just prior to sampling, given as $x_x(t)$, has the following general form,

$$x_x(t) = \sum_{n=1}^{N} a^0(nT)h_{x_x}^0(t-nT) + \sum_{l=1}^{L}\sum_{n=1}^{N} a^l(nT)h_x^l(t-nT-\zeta^l) + p_t(t) * p_r(t) * n_x(t). \quad (5.29)$$

where N is the number of symbols transmitted during the observation period, L is the number of co-channel interferers (assumed constant over the observation time), ζ^l is a delay associated with the l^{th} interferer, a_n are the possibly complex transmitted symbols,

$n_x(t)$ is the AWGN for the x^{th} antenna, and $h_x^0(t-nT)$ and $h_x^l(t-nT-\zeta^l)$ are the pulses received from the desired and l^{th} interferer respectively given by,

$$h_x^i(t) = p_t(t) * g_x^i(t) * p_r(t), \qquad i= 0,1,2,....L \qquad (5.30)$$

where $p_t(t)$ and $p_r(t)$ are the transmit pulse and receive pulse respectively, and $g_x^i(t)$ is the channel response between the i^{th} user and the x^{th} antenna.

If in Equation 5.14 it is assumed that the channel is frequency-flat, $g_x^i(t)$ takes the simple form given by,

$$g_x^i(t) = \alpha_x^i \delta(t), \qquad (5.31)$$

where α_x^i is a complex variable whose statistics are dependent on the channel model that is assumed.

In all the work presented in this thesis the IS136 standard has been used to model the digital communication system analyzed. In IS136, both transmit and receive filters are specified. The output from the convolution of these two filters is a Nyquist pulse, therefore the expression in Equation 5.30 can be re-written to include both the transmit and receive filters such that,

$$h_x^i(t) = N_{yq}(t) * g_x^i(t). \qquad (5.32)$$

where $N_{yq}(t)$ is a Nyquist pulse, which is normalized so that $N_{yq}(0)$ is equal to one.

If the output of the x^{th} receive filter is sampled at the symbol rate T_s^{-1} (we have assumed perfect symbol timing between the transmitter and the receiver) the expression in Equation 5.29 becomes, assuming the same delay profile at each antenna,

$$x_x(mT) = \sum_n a^0(nT) h_x^0(mT - nT) + \sum_{l=1}^{L} \sum_{n=1}^{N} a^l(nT) h_x^l(mT - nT - \zeta^l) + n_x(mT), \quad (5.33)$$

where ζ^l has been constrained to be $\in$ (0, T_s), and the delay profile at each antenna to be the same.

The first term on the RHS of Equation 5.33 is in the form of a discrete time convolution. Using Equation 5.32, and Equation 5.14 the desired user's composite channel response at antenna x as can be given as ,

$$h_x^o(mT) = p(t) * \sum_j \alpha_{x,j}^0 \delta(t - \tau_j)_{t=mT} = \sum_j \alpha_{x,j}^0 p(mT - \tau_j) \quad (5.34)$$

Where $p(t) = N_{yq}(t)$, and the width of the discrete channel is assumed to be finite such that the variable "*m*" extends from +K to –K, a reasonable assumption given the shape of the pulse $p(t) = N_{yq}(t)$. A similar argument can be made for the interference term, and the expression in Equation 5.33 can be re-written as,

$$x_x(mT) = \left[a^0(nT) * h_x^0(nT) + \sum_{l=1}^{L} a^l(nT) * h_x^l(nT) \right]_{n=m} + n_x(mT) \quad (5.35)$$

Now the term $x_x(mT)$ can be expressed as the summation of two discrete time convolutions and additive white Gaussian noise. Given that the noise at the input to the receive filter is white, the filtered noise will also be white since the correlation between two Ts-spaced samples of the receive filter is zero.

Given the expression for the envelope in Equation 5.11 and the properties for the frequency response of its' base-band components given by Equation 5.28 along with the discussion in section 5.5.1, each multi-path wave's envelope can be formed using the method shown below in Figure 5.9.

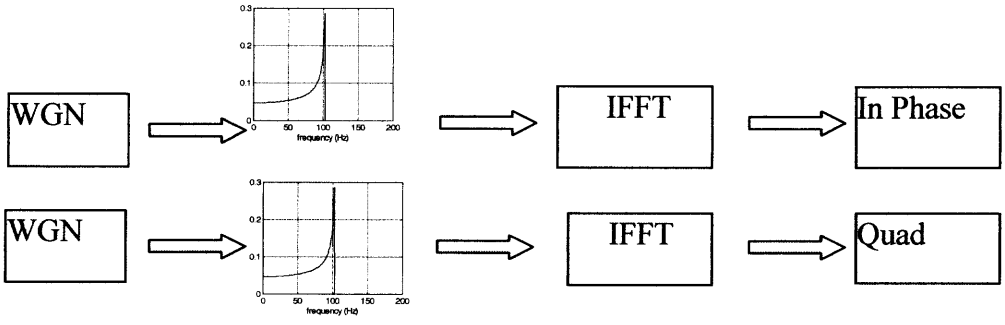

Figure 5.9 Creation of in-phase and quadrature components for Rayleigh weights.

Using this method, two iid, white Gaussian noise processes are formed and each is individually filtered using the response given by Equation 5.28). This gives each component the right correlation properties. The output from each filter is then inverse transformed to give the in-phase and quadrature terms in Equation 5.11. Shown below in Figure 5.10 is a typical spectrum at the input to an IFFT block taken during a simulation run. It comes very close to the theoretical spectrum given in Figure 5.7. To get insight into the time domain properties of the simulated envelopes the covariance function taken at the output from the IFFT block is also shown.

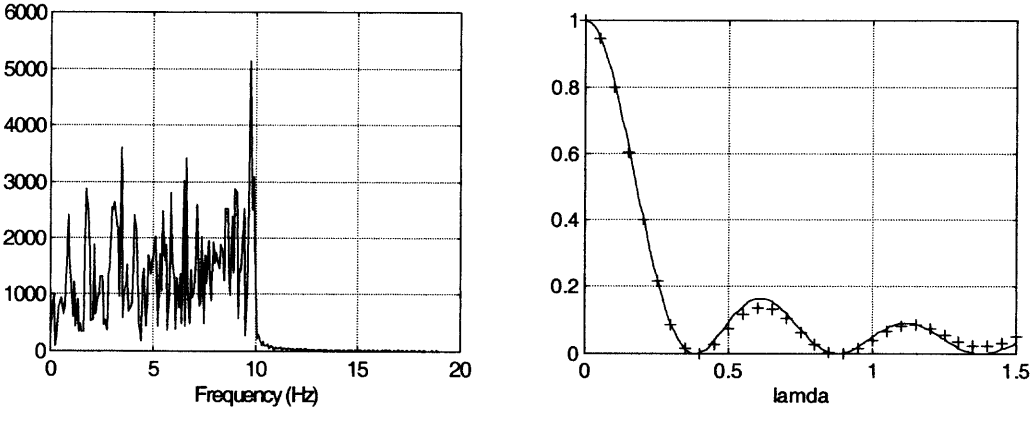

Figure 5.10 Spectrum of base-band components for a f_{max} of 10 Hz (left), and covariance function.

The "+" marks in the figure are the theoretical covariance function given by Equation 5.21). The results show a very close match between both measured and theoretical functions.

To verify the statistical properties of the simulator two histograms have been compiled, taken from two hundred thousand samples, they appear in Figure 5.11. Included in the graphs, shown as the solid curve, are the theoretical expressions given by Equation 5.12, and 5.13.

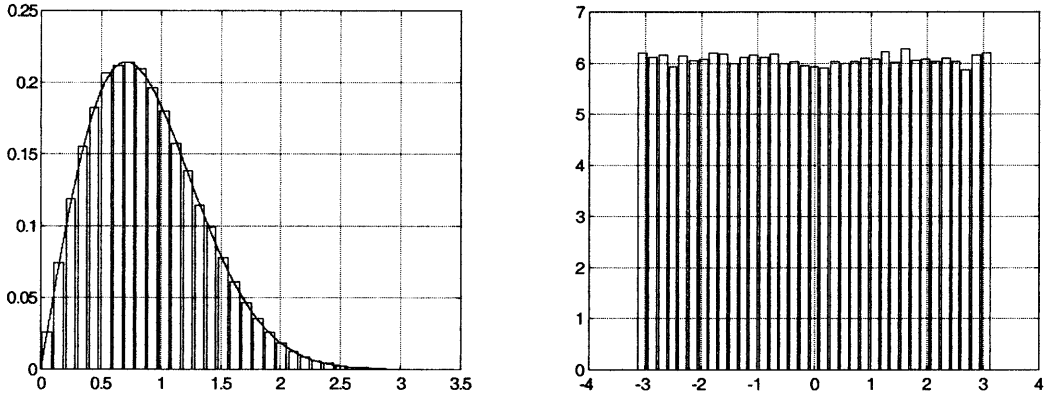

Figure 5.11 PDF's of the simulated fading envelope (left), and phase (solid lines are the theoretical values).

Included below are addition graphs which show the covariance functions of both the phase and envelope over the period of one IS136 TDMA frame. The solid line in the graphs is for a fading rate of one hundred, and eighty Hertz, which for PCS frequencies is approximately highway speed (~ 60 Mph). The dashed line represents, again for PCS frequencies, a fading rate of ten Hertz, or walking speed (~3 Mph).

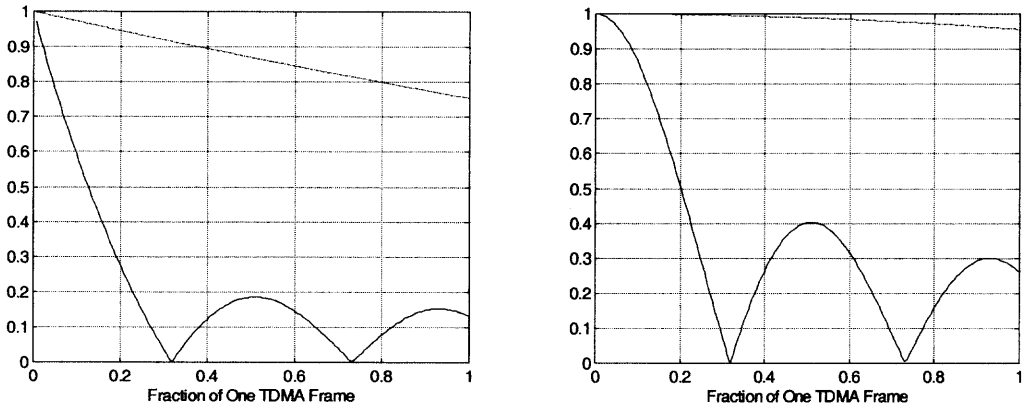

Figure 5.12 Normalized covariance functions of phase (left), and envelope, over one TDMA frame.

This has been done to illustrate why the simulations presented in this work have been simplified by making the assumption that the envelope and phase of the fading signals are constant over one IS136 TDMA bust, approximately seven milliseconds long. From Figure 5.12, it's obvious that a time-flat fading model would not be appropriate for highway speeds. The model is more suitable for walking speed, approximately three miles-per-hour, since both envelope and phase are stay highly correlated over the length of a data burst. By using the time-flat fading for all the simulations presented in this thesis, a walking speed for the mobile user is implied. For completeness, sample functions from the simulator of the signal envelope and cross correlation of the Rayleigh coefficients are shown below.

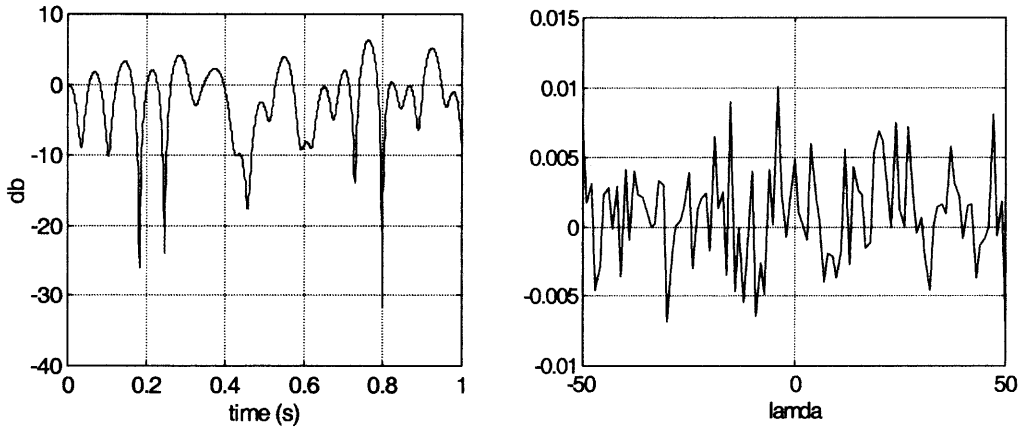

Figure 5.13 Actual Rayleigh fading envelope for f_{max} of 10 Hz (left), and measured cross covariance of multi-path ray envelopes.

5.3 Results

Additional results from simulations have been included, and are presented below. These simulations are for the standard two-ray multi-path user channel with inter-ray delay of half a symbol period. Even though, in the literature most authors like to use the one symbol delay model for the user's channel, the results are much too favorable when a MLSE is used in the receiver. This is because the MLSE can achieve better performance through time diversity. Since as shown in Figure 5.13, each multi-path ray fades independently, the MLSE will achieve time diversity through it's metric calculations. For convenience the metric variables from Chapter 3 have been reproduced below in Equation 5.36 and Equation 5.37,

$$S_{n-m} = \int_I h(t - nT)h^*(t - mT)dt \tag{5.36}$$

$$Z_n = \int_I R(t)h^*(t - nT)dt \ . \tag{5.37}$$

When Equation 5.14 is inserted, for a two-path channel, into Equation 5.36 we obtain,

$$S_{n-m} = \int_I \sum_i \sum_j \alpha_{x,j}^0 \alpha_{x,i}^{*0} p(t-nT-\tau_j)p(t-mT-\tau_i)\ dt, \quad i,j=0,1. \tag{5.38}$$

Which, for $n\text{-}m=0$ is us the following result;

$$S_0 = \int_I \left|\alpha_{x,0}^{*0}\right|^2 p(t)p(t)\ dt + 2\int_I \alpha_{x,1}^0 \alpha_{x,0}^{*0} p(t-\tau_1)p(t)\ dt + \int_I \left|\alpha_{x,1}^{*0}\right|^2 p(t-\tau_1)p(t-\tau_1)\ dt, \tag{5.39}$$

$$S_0 = \left|\alpha_{x,0}^{*0}\right|^2 \rho(0) + \left|\alpha_{x,1}^{*0}\right|^2 \rho(0) + 2\alpha_{x,1}^0 \alpha_{x,0}^{*0} \int_I p(t-\tau_1)p(t)dt, \tag{5.40}$$

where,

$$\rho(\tau) = \int_I p(t)p(t-\tau)dt. \tag{5.41}$$

is the pulse correlation function. A plot of this function, for an IS136 system is shown below.

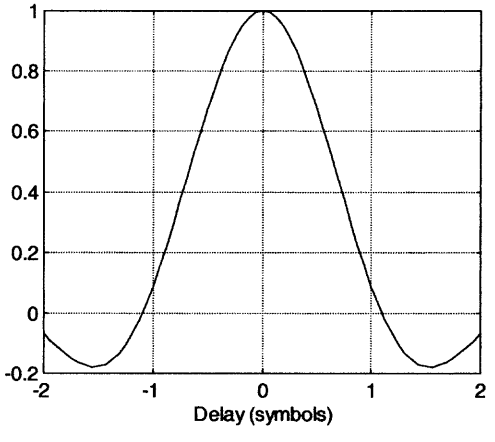

Figure 5.14 Pulse correlation function for IS136 system.

Note that the pulse correlation function becomes smaller as τ becomes larger, and for $\tau = T_s$ the function is very small. The first and second terms in Equation 5.40 show how diversity is obtained within the transition metric. Only the third term can reduce the diversity gain, so if that term is small than its' effect on the diversity gain will be negligible. On the other hand if the term is large, as might be the case when τ is small than the effect of this term on the diversity gain cannot be discounted. This is why two-path channel with an inter-ray delay of one symbol will result in better overall performance. The same argument as that mentioned above also applies to the other metric variables given by Equation 5.36 and Equation 5.37. A plot of the effect of inter-ray delay on performance is given below for a channel with no co-channel interferer.

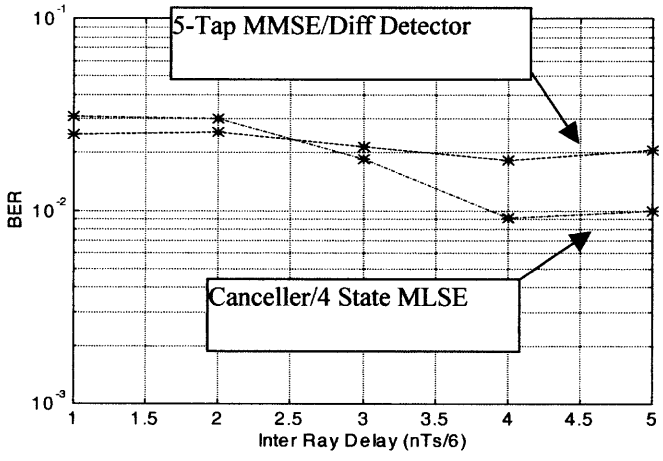

Figure 5.15 Effect of inter-ray delay on performance.

The graphs presented below show that, as expected, the performance of the Canceller/MLSE degrades when the inter-ray delay is reduced. The results presented in Figure 5.16 are for a two-antenna single element canceller and reduced inter-ray delay of half of a symbol length. Comparing the results of the symbol-spaced channels shown in

Figure 4.3 and Figure 4.4, it is obvious that the performance degrades by an order of magnitude. The legend for Figure 5.16 is as follows; + = a single antenna, o = Canceller/Differential Detector with $b = [0\ 1\ 0]^T$, * = Canceller/Differential Detector with b = c, x = single tap Optimum Combiner/Differential Detector.

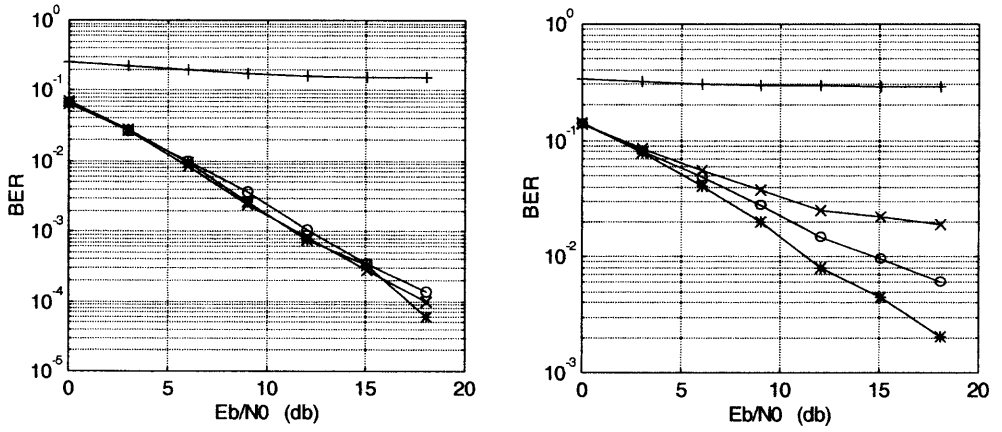

Figure 5.16 Performance of receivers for a two-path channel with inter-ray delay of Ts/2, and no interferer (left) or one equal power, flat-faded interferer.

The results shown in Figure 5.16 and Figure 5.17 are for a two-element canceller with five temporal taps on each element, and a constraint on the estimator, limiting the result to only two causal taps. By comparing the results to Figure 4.11 and Figure 4.12, one can see that when two additional temporal taps are added to each antenna, the performance degradation due to the Ts/2 channel is nullified.

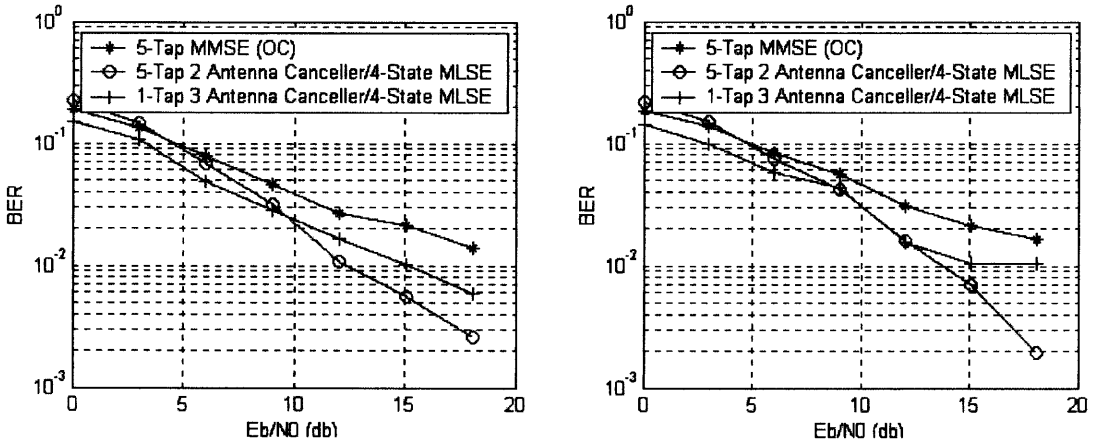

Figure 5.17 Performance for a two-path Ts/2-spaced channel with one equal power interferer with a two-path Ts-spaced channel (left) and a three-path Ts/2-spaced channel.

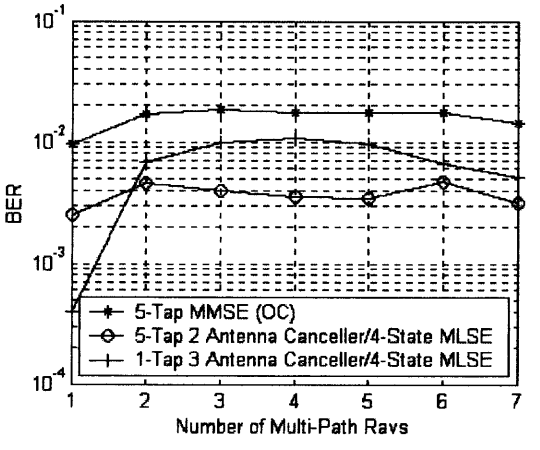

Figure 5.18 The addition of multi-path components to one equal power interferer for a two path, $T_{s/2}$-spaced channel with Eb/N_0= 17 db.

REFERENCES

1. M. Leou, C. Yeh, "A Novel Hybrid of Adaptive Array and Equalizer for Mobile Communication," *IEEE Trans. Veh. Technol.*, vol. 49, pp. 1-10, Jan. 2000.

2. J. H. Winters, "Signal Acquisition and Tracking with Adaptive Arrays in the Digital Mobile Radio System IS-54 with Flat Fading," *IEEE Trans. Veh. Technol.*, vol. 42, pp. 377-384, Nov. 1993.

3. G. Ungerboeck, "Adaptive Maximum-Likelihood Receiver for Carrier-Modulated Data-Transmission Systems," *IEEE Trans.On Communications,* com-22, pp. 624-635, May 1974.

4. J. H. Winters, "Optimum Combining in Digital Mobile Radio with Co-channel Interference," *IEEE Journal on Selected Areas in Comm.*, vol. Sac-2, pp. 528-539, July 1984.

5. J. H. Winters, Sirikat Lek Ariyavisitakul, Inkyu Lee, "Optimum Space-Time Processors with Dispersive Interference: Unified Analysis and Required Filter Span," *IEEE Trans. On Comm.*, vol. 47, pp. 1073-1083, July 1999.

6. J. H. Winters, Ye Li, Nelson R. Sollenberger, "Spatial-Temporal Equalization for IS-136 TDMA Systems with Rapid Dispersive Fading and Co-channel Interference," *IEEE Trans. Veh. Technol,* vol. 48, pp. 1182-1194, July 1999.

7. D. A. George, "Matched Filters for Interfering signals," *IEEE Trans. On Info Theory,* pp. 153-154, Jan. 1965.

8. G. D. Forney Jr., "Maximum-Likelihood Sequence Estimation of Digital Sequences in the Presence of Intersymbol Interference," *IEEE Trans. On Info Theory.*, vol. IT-18, pp. 363-378, May 1972.

9. B. R. Peterson, D. D. Falconer, "Exploiting Cyclostationary Subscriber-Loop Interference by Equalization," *in Conf. Rec. IEEE GLOBECOM'90* , San Diego, CA, Dec. 2-5, 1990, vol. 2, pp. 1156-1160.

10. ---------, "Minimum Mean Square Equalization in Cyclostationary and Stationary Interference-Analysis and Subscriber Line Calculations," *IEEE Journal On Selected Areas in Comm.*, vol. 9, pp. 931-940, August 1991.

11. P. Balaban, J. Salz, "Dual Diversity Combining and Equalization in Digital Cellular Mobile Radio," *IEEE Trans. Veh. Technol.*, vol. 40, pp. 342-354, May 1991.

12. ---------, "Dual Diversity Combining and Equalization in Digital Cellular Mobile Radio: Theoretical Considerations," *IEEE Trans.On Communications,* vol. 40, pp. 886-894, May 1992.

13. M. Schwartz, "Abstract Vector Spaces Applied to Problems in Detection and Estimation Theory," *IEEE Trans. On Info. Theory,* vol. IT-12, pp. 327-336, July 1966.

14. G. E. Bottomley, S. Chennakeshu, "Unification of MLSE Receivers and Extension to Time-Varying Channels," *IEEE Trans. On Comm.,* vol. 46, pp. 464-472, April 1998.

15. W. Sheen, G. L. Stuber, "MLSE Equalization and Decoding for Multi-path-Fading Channels," *IEEE Trans.On Communications,* vol. 39, pp. 1455-1464, Oct. 1991.

16. Q. Liu, Yongbing Wau, "A Unified Detection Technique for TDMA Digital Cellular Radio," 43rd *IEEE Veh. Technol Conf.,* Secaucus, NJ, pp. 265-268, May 18-20 1993.

17. E. Villier, "Performance Analysis of Optimum Combining with Multiple Interferers in Flat Rayleigh Fading," *IEEE Trans. On Comm.,* vol. 47, pp. 1503-1510, Oct. 1999.

18. J. Zhaung, V. A. Aalo, "Performance of Antenna Array Systems with Optimum Combining in a Rayleigh Fading Environment," *IEEE Communications Letters,* vol-4, pp. 387-389, Dec. 2000.

19. G. E. Bottomley, Karim Jamal, "Adaptive Arrays and MLSE Equalization," *in Proc. VTC '95*, Chicago, Il., pp. 25-28, July 25-28 1995.

20. G. E. Bottomley, K. Molnar, S. Chennakeshu, "Interference Cancellation with an Array Processing MLSE Receiver," *IEEE Trans. Veh. Technol.,* vol. 48, pp. 1321-1331, Sept. 1999.

21. G. E. Bottomley, K. Molnar,"Adaptive Channel Estimation for Multi-channel MLSE Receivers," *IEEE Communications Letters,* vol. 3, pp. 40-42, Feb. 1999.

22. T. D. Pham, K. G. Balman, "Multi-path Performance of Adaptive Antennas with Multiple Interferers and Correlated Fadings," *IEEE Trans. Veh. Technol.,* vol. 48, pp. 342-352, March 1999.

23. K. Scott, E. B. Olasz, A. Sendyk, "Diversity Combining with MLSE Equalization," *IEE Proc.-Communications,* vol. 145, pp. 105-108, April 1998.

24. W. C. Jakes, *Microwave Mobile Communications*, IEEE Press, Piscataway, N.J. 1994.

25. J. G. Proakis, *Digital Communications*, McGraw-Hill, New York, N.Y., third ed., 1995.

26. Y. Bar-Ness, "Adaptive Array Processing and Interference Cancellation," *IEEE Vehicular Technology Tutorial*, Delft University of Technology, January 1994.

27. S. P. Applebaum, "Adaptive Arrays," *IEEE Trans. Antennas and Propagation,* vol. AP-24, No. 5, pp. 585-598, Sept. 1976.

28. H. L. Van-Trees, *Detection, Estimation and Modulation Theory Part III*, John Wiley and Sons, New York, N.Y., 1968.

29. S. O. Rice, "Mathematical Analysis of Random Noise," *Bell System Tech. J. 23,* pp. 282-332, July 1944.

30. S. O. Rice, "Statistical Properties of a Sine Wave Plus Random Noise," *Bell System Tech. J. 27,* pp. 109-157, January 1948.

31. A. Abdi, "Class Notes for Special Topics Class ECE789," New Jersey Institute of Technology, Newark NJ, Spring 2002.

32. R. H. Clarke, "A Statistical Theory of Mobile Radio Reception," *Bell System Tech. J. 47*, pp. 967-1000, July 1968.

33. W. C. Y. Lee, *Mobile Cellular Telecommunications*, McGraw-Hill, New York, N.Y. second ed., 1995.